ANDRÉ CARVALHO LIMA

More Than Supportive: Liana Attachment to Supports Lead to Profound Changes in Xylem Anatomy, Hydraulic Conductivity and Cambium Transcriptional Profile

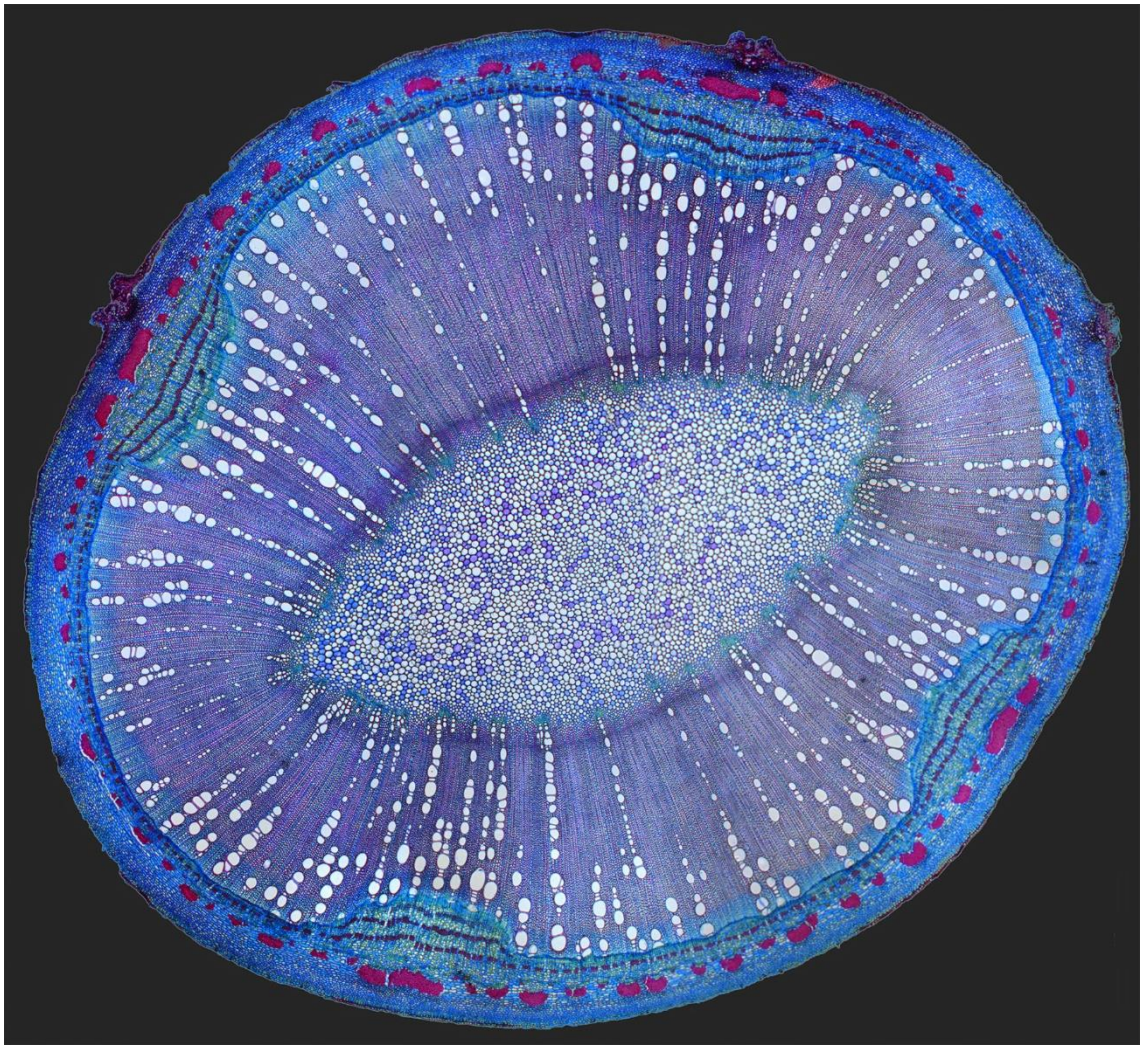

São Paulo
2020

ANDRÉ CARVALHO LIMA

Mais do que um apoio: a conexão da uma liana a suportes leva a profundas mudanças na anatomia do xilema, de condutividade hidráulica, e do perfil transcricional do câmbio

More Than Supportive: Liana Attachment to Supports Lead to Profound Changes in Xylem Anatomy, Hydraulic Conductivity and Cambium Transcriptional Profile

Tese apresentada ao Instituto de Biociências da Universidade de São Paulo, para a obtenção de Título de Doutor em Ciências. Programa: Ciências Biológicas (Botânica).

Orientadora: Profa. Dra. Veronica Angyalossy

Coorientadora: Profa. Dra. Magdalena Rossi

São Paulo
2020

Ficha catalográfica

Lima, André Carvalho 2020

Mais do que um apoio: a conexão da uma liana a suportes leva a profundas mudanças na anatomia do xilema, de condutividade hidráulica, e do perfil transcricional do câmbio
73 páginas

Tese (Doutorado) - Instituto de Biociências da Universidade de São Paulo. Departamento de Botânica.

1. Xilema 2. Xilogênese 3. Transcriptoma
4.Anatomia funcional 5. Condutividade hídrica
I. Universidade de São Paulo. Instituto de Biociências. Departamento de Botânica.

Comissão Julgadora:

_____	_____
Prof(a). Dr(a).	Prof(a). Dr(a).
_____	_____
Prof(a). Dr(a).	Profa. Dra.Veronica Angyalossy Orientadora

Por tudo, por cada segundo juntos, por cada gesto e cada sorriso, por cada momento feliz ou triste, que invariavelmente foram mais felizes do que teriam sido de qualquer outra forma, dedico esse trabalho à Bruna.

Agradecimentos

À Universidade de São Paulo, ao Instituo de Biociências, e ao Laboratório de Anatomia Vegetal, pelo apoio em tantos anos de convívio.

À Coordenação de Aperfeiçoamento de Pessoal de Nível Superior – CAPES, e ao Conselho Nacional de Desenvolvimento Científico e Tecnológico - CNPQ pelas bolsas e auxílios concedidos.

À Bruna Rodrigues Ferreira, pelo amor, carinho, compreensão, paciência. Pela convivência, pelo apoio, pelo sorriso e pelo choro. Por cada segundo juntos, que já tivemos e pelos que ainda teremos.

Ao meus pais, Claudia da Costa Carvalho Lima e José Ricardo Moreira Lima, por todo o amor e apoio. Quão grandes eles são. Aos meus irmãos Tiago C. Lima e Rafael C. Lima por sempre ao meu lado por todos esses anos. Às Mariana Antunes e Andréa Valente pelo convívio e pelos meus sobrinhos queridos. À Izabel C. Couceiro, minha terceira irmã.

À minha orientadora Veronica Angyalossy, por todos esses anos de tantos aprendizados. Por ser um modelo de professora e de pessoa.

À minha coorientadora Magdalena Rossi, por ter me recebido tão calorosamente, por ter aceitado essa empreitada, por todo o apoio e compreensão, que se tornou também um modelo de pesquisadora, profissional e de pessoa.

Aos Verônicos e Verônicas pelo convívio, pela amizade, e pelos saberes compartilhados, que vão muito além da botânica. Muito obrigado ao Israel Neto, Camila Monje, Marina Milanello, Erica Moniz, Lui Teixeira, Ricardo Chinen, Carolina Bastos, Mariana Victório, e em especial ao Caian Gerolamo e ao Marcelo Pace. Aos demais Veronicos que não cito diretamente aqui, mas guardo no coração.

À colegas, amigas e grandes cientistas Daniele Rosado e Paula Elbl pela ajuda e momentos de descontração. Aos colegas Giuliano Locosseli e Mariane de S. Baena por conversas e trocas.

Ao amigo Erismaldo Carlos de Oliveira, por todo cuidado com minhas plantas e com o jardim do IB – USP

Às amigas e melhores técnicas Gisele Costa, Tássia dos Santos e Paula Jardim, por todo apoio e paciência.

Aos professores do Laboratório de Anatomia Vegetal Gladys Flávia Melo de Pina, Gregório Ceccantini Diego Demarco, e em especial à Nanuza Luiza de Menezes.

Ao amigão Antônio Carlos Barbosa, por todo o conhecimento transmitido, alegria e amizade.

À minha nova família, que me recebeu com tanto amor e carinho, os Rodrigues e Ferreiras, Vera, Sergio, Laura, Ana, Angela, Lu, Preta, João, Nega, Marcelo, Mirian, Gael, Glória, Dani, Lígia.

Ao Paulo Cseri e ao Rafael da Silva Cruz pelo convívio, ideias e discussões, científicas ou não.

Aos grandes amigos da turma de 2004 do Curso de Ciências Biológicas. Por todo o crescimento que passamos juntos, na ciência e na vida. Um obrigado especial ao Leonardo Jo, André Vaquero e ao Guilherme Cruz pelas inúmeras conversas, mas algumas em específico que me ajudaram muito a delimitar melhor minha pesquisa. Obrigado Base, Vaquero, Musquito, Ju, Bolotinha, Mari, Burzun, Thalita Fer, Xurrus, Estela, Rafa, Rena, Ro, Carioca, Drika, Piru, Marina, Albieri, Bigodes, Laura, Debora, Lucimara, Puera, Xampu, Mamilo, Lui, Pato, Mamão, Taiji, Ruggero, Alma, Priscila, Sassa, Maíra, Alice, Vivi, Nayara, Jundi... Escrevendo cada nome milhares de lembranças me veem à mente. Queria ter o tempo, espaço e forças para fazer agradecimentos específicos a cada um de vocês.

Aos amigos da turma de 2007 do Curso de Ciências Biológicas: Alê, Yoshi, Errô, Joseph, Crote, Hana, Samurai, Gê, Preps, Flavião, Flávio, Coifa, Gustavo Duffner de Almeida, Cassis, Bolshoi, Semvê, Mica, Toshiba, Pira, Amarula, Esparta, Bowie, Wally, Cinthia, Iha, Leo, Frito.

Índice

Apresentação

A presente tese está editorada e parcialmente formatada na forma de artigo a ser submetido à revista *New Phytologist* com o seguinte título e autores:

More Than Supportive: Liana Attachment to Supports Lead to Profound Changes in Xylem Anatomy, Hydraulic Conductivity and Cambium Transcriptional Profile

André C Lima[1], Sónia CS Andrade[2], Caian S Gerolamo[1], Diego T de Souza[1], Ricardo Chinen[1], Horácio Montenegro[3], Luiz L Countinho[3], Magdalena Rossi[1], Veronica Angyalossy[1]

[1]Botany Department, Biosciences Institute, University of São Paulo, No 277, Rua do Matão, 05508-090, Cidade Universitária - São Paulo – SP, Brazil. [2] Genomic Diversit Laboratory, Genetics and Evolutionary Biology Department, Biosciences Institute, University of São Paulo, No 277, Rua do Matão, 05508-090, Cidade Universitária - São Paulo – SP, Brazil. [3] Genetics Department, Luiz de Queiroz College of Agriculture, No 11, Pádua Dias Av., Cidade Universitária, 13400-970 - Piracicaba, SP - Brasil

Resumo

• O xilema secundário desempenha duas funções cruciais: o suporte mecânico e condução de água e minerais. Muitas lianas mostram duas fases anatômicas contrastantes em seu xilema, uma inicial, onde o xilema é homogêneo, fibroso e apresenta vasos de pequeno diâmetro, denominada xilema autoportante, e posteriormente o xilema lianescente, anatomicamente complexo, com vasos grandes e dimórficos e menos tecido de suporte. Não se sabe, no entanto, o que leva à mudança abrupta da formação do xilema.

• Neste estudo, abordamos as questões de o que inicia e quais são os determinantes genéticos das profundas mudanças durante a transição do xilema autossuporte para o xilema lianescente na liana *Bignonia magnifica*, Bignoniacae. Para esse fim, analisamos primeiramente as taxas de crescimento de plantas cultivadas com e sem suportes, como os parâmetros hidráulicos variavam ao longo do caule e descrevemos em detalhes a anatomia do xilema autossuportante e lianescente. Em seguida, construímos o transcriptoma do câmbio e do xilema em diferenciação dessas duas fases e realizamos uma análise de expressão diferencial dos dados gerados por RNA-Seq.

• Nosso trabalho mostra que a presença de suportes leva a alterações no padrão de crescimento e nos parâmetros anatômicos ao longo do caule, aumentando a condutividade potencial e promovendo a formação de xilemas lianescentes. Essas alterações estão associadas à expressão diferencial de genes relacionados à divisão celular e à biossíntese da parede celular, sobre-expressos na fase autoportante, e de fatores de transcrição, defesa / morte celular e genes responsivos a hormônios, sobre-expressos na fase lianescente.

• Concluímos que a anatomia mais complexa na fase lianescente é o resultado de uma regulação transcricional mais complexa no câmbio e xilema em diferenciação.

Palavras-chave: xilema; xilogênese; transcriptoma; anatomia funcional; condutividade hídrica

Summary

- Secondary xylem performs two crucial functions, namely mechanical support and water and mineral conduction. Many lianas show two contrasting xylem anatomy phases, the initial homogeneous, fibrous and small vesselled self-supporting xylem, and the later lianescent xylem, which is anatomically complex, with large and dimorphic vessels and less supportive tissue. It is not known, however, what leads to the abrupt change of xylem formation.
- In this study, we address the question of what triggers and which are the genetic determinants of the profound changes during the transition from self-supporting to the lianescent xylem in the liana *Bignonia magnifica*, Bignoniacae. For this purpose, we first analyzed growth rates of plants grown with and without supports, how hydraulic parameters varied along the stem and described in detail self-supporting and lianescent xylem anatomy. We then constructed cambium and differentiating xylem transcriptome of these two phases and conducted a differential expression analysis of RNA-Seq generated data.
- Our work shows that the presence of supports leads to changes in growth pattern and anatomical parameters along the stem, increasing potential conductivity, and promotes lianescent xylem formation. These changes are associated to differential expression of genes related to cell division and cell wall biosynthesis, overregulated in self-supporting phase, and of transcription factors, defense/cell death, and hormone-responsive genes, overregulated in lianescent phase.
- We conclude that the more complex anatomy in lianescent phase is the result from a more complex transcriptional regulation in cambium and wood forming tissues.

Keywords: xylem; xylogenesis; transcriptome; functional anatomy; hydraulic conductivity.

Introduction

Secondary xylem, or simply wood, performs two crucial functions for woody plants survival and reproductive success: mechanical support, optimizing light uptake for photosynthesis and exposure of reproductive organs; and the conduction of water and nutrients from the soil and between source and sink organs, serving yet as storage tissue during unfavorable periods (Baas *et al.*, 2004). In contrast to the homogeneous, almost entirely tracheid composed gymnosperm wood, cellular specialization evolution in angiosperm xylem led to a division of labor among the different cell types composing it, with support being carried out by fibers, conduction of water and minerals carried out mainly by vessels, and storage by axial and radial parenchyma (Bailey & Tupper, 1918; Tyree & Zimmermann, 2002; Evert, 2006). Despite the established relationship of cell types and their functions, there is a great diversity of arrangements, compositions and dimensions of these cell types in the xylem of plants. In turn, this anatomical structural diversity are under genetic control , which regulation has been unveiled with the studies in model species such as *Arabidopsis thaliana* and *Populus* (J. Zhang *et al.*, 2014; Ye & Zhong, 2015; Sundell *et al.*, 2017; J. Zhang *et al.*, 2019), and define how plants cope with the different functions (Zieminska *et al.*, 2013; 2015; Beekman, 2016). Overall, relations between genetic control, anatomy structure and functional implications are still poorly understood for wood plants.

Mechanical properties of fibers are controlled by the cell wall thickness, cell wall/lumen ratio (Zieminska *et al.*, 2013), as well as by cell wall hemicellulose and lignin composition, and cellulose amount and microfibril angle (Bergander & Salmén, 2002; Li *et al.*, 2009; MacMillan *et al.*, 2010; Bourmaud *et al.*, 2013). Water conductivity (*K*), in turn, is directly related to vessels diameter (*D*) raised to the fourth power and inversely related to the length (*L*) that the water must travel between roots and leaves. The relation

of K with D^4 shows that even small increments of diameter profound considerable impacts on conductivity, while growth in L could lead to smaller water supply for distally located leaves and limitation in length growth due to an increase in conductivity resistance (Petit & Anfodillo, 2009; Anfodillo *et al.*, 2013). However, the increase of vessels diameter found along the stem allows for a compensatory effect on the path length resistance (West *et al.*, 1999), an hypothesis that was further reinforced by later works (Becker *et al.*, 2000; Sperry *et al.*, 2012). Olson *et al.* (2014), analyzing the stem xylem anatomy at the base and at the top of 257 angiosperm species, found a vessel widening ratio of $D = L^{0.22}$, independent of habit and habitats. This proportion between L and D describes a fast growth in diameter near the apex and a progressive lesser increase toward the base, and its value is consistent with previous models (Becker *et al.*, 2000). The controversy, as well as the insight, of the model lies in the assumption that length in the main factor, if not the only one, determining vessel diameter.

Nevertheless, different proportions of the different cell types that compose secondary xylem may lead to changes in stem properties and how they cope with support and conductivity (Zieminska *et al.*, 2013; 2015; Bittencourt *et al.*, 2016; Gerolamo *et al.* unpublished). Lianas, or woody vines, are an extreme example of reduced amount of supporting cells, namely xylem fibers, that accompanied the evolution of this life form, which uses other plants as supports. Although this iconic component of tropical forests has evolved several times in different groups (Gentry, 1991; Angyalossy *et al.*, 2015), the life form shows a series of striking converging anatomical features, as the presence of huge vessels, up to 500 micrometers in diameter (Angyalossy *et al.*, 2015), that are associated with small vessels (vessel dimorphism, Carlquist, 1981). Moreover, the reduction of fibers and increase of parenchyma in comparison to phylogenetically related species, and the presence of cambial variations, that are different arrangements of

secondary vascular tissues (Carlquist, 1985; 2001; Angyalossy *et al*., 2012) are characteristic of lianescent habit. All these features are collectively called lianescent vascular syndrome (Angyalossy *et al.*, 2015) and are observed in both existing and extinct liana species (Burnham, 2009).

Nevertheless, many lianas show a denser xylem at the beginning of their development, which is more fibrous and shows smaller vessels, resembling the xylem of self-supporting species (Schenck, 1893; Obaton, 1960; Caballé, 1998; Gallenmuller *et al.*, 2001). The transition from this denser xylem phase (termed as self-supporting xylem hereafter) to that showing the lianescent vascular syndrome (named as lianescent xylem hereafter) occurs abruptly, as seen in the adult stem cross-section (Fig. 1), and was observed in 85 % of the more than 13,000 specimens, belonging to 400 liana species of 50 different families analyzed by Caballé (1998). The beginning of lianescent xylem production occurs, in different stems, after the formation of different amounts of the self-supporting xylem (Caballé, 1998), which suggests that it is not as a result of a pre-defined developmental program. It is not known, however, what leads to the abrupt change of xylem formation (Rowe & Speck, 1996; Caballé, 1998). While several reports have investigated the exuberant anatomical architectures formed due to cambial variants (Rajput *et al.*, 2008; Pace *et al.*, 2009; Tamaio *et al.*, 2010; Cabanillas *et al.*, 2017), the sudden change in lianas xylem anatomy has been poorly addressed (Obaton, 1960; Caballé, 1993; 1998; Gallenmüller et al., 2001). The detailed characterization of the two anatomy phases, not only contributes to the better understanding of the control of their formation, the demands suffered and met by lianas xylem and the evolution of this important life form, but also shed light on factors that modulate the development of

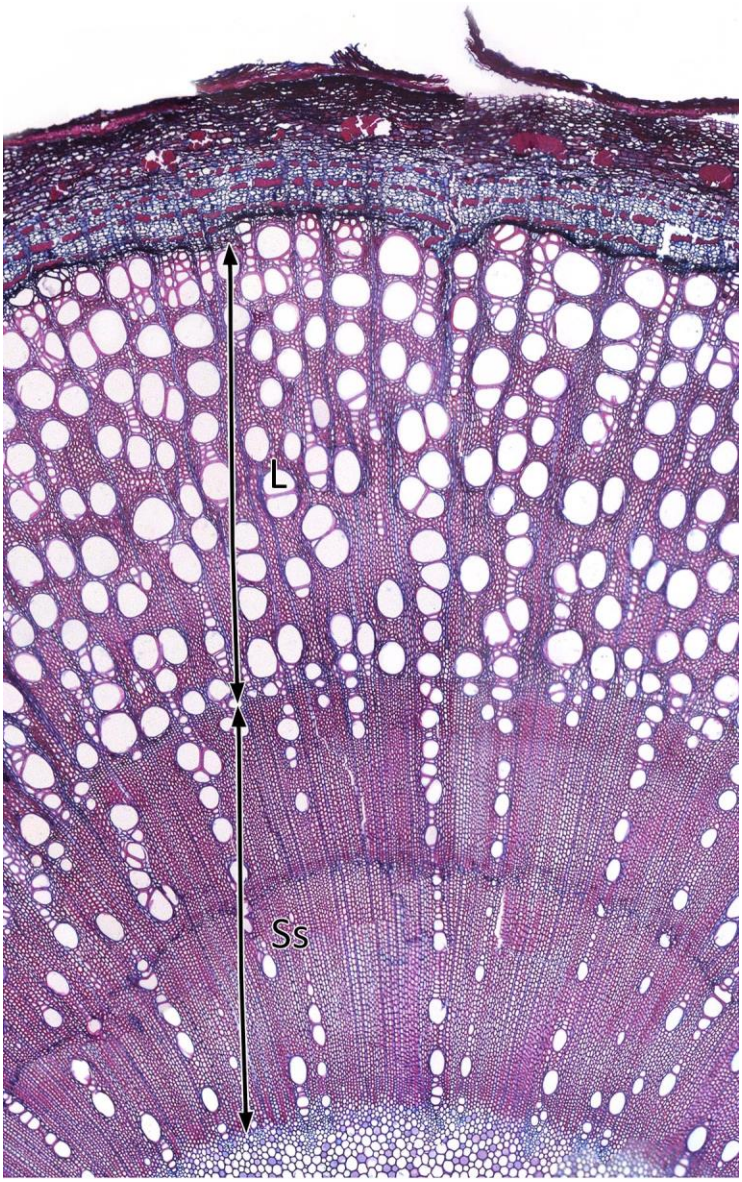

Fig. 1. *B. magnifica* stem cross section. As *B. magnifica*, many lianas show the formation of a denser xylem at the beginning of the secondary growth, composed by a high proportion of fibers and with small vessels, denominated here self-supporting xylem (**Ss**), and a sudden change to a xylem showing the lianescent vascular syndrome, *i.e.* with less fibers and large vessels, which are associated with small vessels, denominated lianescent xylem (**L**).

secondary xylem, with underlying genetic traits and the implications for hydraulic conductivity and mechanical performance, in plants as a whole.

The use of model species, as *Arabidopsis thaliana* and *Populus*, has provided invaluable advances in the understanding of cambium installation and activity, as well as xylem formation and differentiation (Groover, 2005; Hirakawa *et al.*, 2010; Agusti *et al.*, 2011; Robischon *et al.*, 2011; J. Zhang *et al.*, 2014; 2019; Ye & Zhong, 2015; Sundell *et al.*, 2017). The signaling pathway regulating cambial maintenance and proliferation is conserved from herbaceous to woody species, as described in both *A. thaliana* and *Populus*, and is controlled by the module TDIF/CLE41/CLE44-TDR/PXY-WOX4 (Zhang *et al.*, 2014). TRACHEARY DIFFERENTIATION INHIBITORY FACTOR (TDIF) peptides, which are products of

the posttranslational process of CLAVATA/EMBRYO SURROUNDING REGION (CLE41 /CLE44) protein are produced in the phloem and perceived in the (pro)cambium by the receptor-like kinase TDIF RECEPTOR/PHLOEM INTERCALATED WITH XYLEM (TDR/PXY). This interaction induces the expression of the *WUSCHEL-RELATED HOMEOBOX* gene (*WOX4*), which in turn regulates cell proliferation (Hirakawa et al., 2010; Etchells & Turner, 2010). Secondary cell wall (SCW) biosynthesis regulation by the primary and secondary master switches NAM/ ATAF1/CUC2 (NAC) and MYB (V-MYB protein from avian myeloblastosis virus) transcription factors, respectively, was also described in *A. thaliana* (Kubo et al., 2005; Zhong et al., 2006; McCarthy et al., 2009; Ko et al. 2009). The elaborated transcriptional network controlling fiber and vessels differentiation was further characterized in numerous other species, such as *Populus trichocarpa*, *Oryza sativa*, *Brachypodium distachyon*, *Eucalyptus grandis* and *Zea maize* (Hu et al., 2010; Nuruzzaman et al., 2010; Valdivia et al., 2013; Soler et al., 2015; Zhong et al., 2011).

Molecular studies in non-model species, on the other hand, have become possible in an unprecedented way thanks to the use of new technologies, such as next-generation sequencing (Wang *et al.*, 2009), and allowed to unravel many unique features and processes absent in model species (Carpentier *et al.*, 2008). In this study, we made an integrative approach to address the question of what triggers and which are the genetic determinants of the profound changes during the transition from self-supporting to the lianescent xylem in the liana *Bignonia magnifica* W.Bull (Bignoniaceae). For this purpose, we first analyzed growth rates of plants grown with and without supports, how xylem parameters varied along the stem, described in detail self-supporting and lianescent xylem anatomy and what are the implications for hydraulic conductivity. We then

constructed cambium and differentiating xylem transcriptome of these two phases and conducted a differential expression analysis of RNA-Seq generated data.

Our work shows that the presence of supports leads to changes in growth pattern and anatomical parameters along the stem, increasing specific conductivity, and promotes lianescent xylem formation. These changes are associated to differential expression of genes related to cell division, cell wall, transcription factors, defense/cell death, and hormone-responsive genes.

Materials and Methods

Plant Material

Bignonia magnifica W. Bull, Bignoniaceae, is native to Central America and northern South America (Lohmann & Taylor, 2014) and is used in ornamentation, showing robust secondary growth early in its development. The species belongs to the monophyletic tribe Bignonieae, the largest tribe of its family and mainly composed by trifoliolated vines, that climb through terminal leaflet modified tendrils. Bignonieae, which has its center of diversity in Brazil (Gentry, 1980), is the most diverse and abundant clade of lianas in neotropical low-land forests (Gentry, 1986) and have been the focus of several studies aiming its anatomy, evolution, hydraulics, ecology, taxonomy, and biomolecules activity (Pace *et al.*, 2011; 2015a,b; 2016; Lohmann *et al.*, 2012; Souza-Baena *et al.*, 2014*a*,*b*; Cordeiro *et al.*, 2017; Duarte *et al.*, 2017; Fonseca *et al.*, 2017; Gerolamo & Angyalossy, 2017; Torres *et al.*, 2018; Beyer *et al.*, 2019; Costa *et al.*, 2019; Kaehler *et al.*, 2019; Thode *et al.*, 2019; Meyer *et al.*, 2020). A synapomorphy of the tribe consists of the formation of four, or multiples of four, wedges of phloem in their stems and roots (Gentry, 1973; Lohmann, 2006; Victorio 2017). These wedges are formed by the differential activity of equidistant portions of the cambium that reduce the production of xylem and

increase the production of phloem, thus being located more internally in the stem than the inter-wedges cambial portions showing regular activity (Dos Santos, 1995; Pace *et al.*, 2009). Xylem anatomy and expression analysis were carried only in the inter-wedges region.

Growth Conditions

In order to avoid intraspecific variation, all analyses and experiments were performed with clones obtained from cuttings of a single plant of *Bignonia magnifica* cultivated at the gardens of the Biosciences Institute of the University of São Paulo, São Paulo (23º S, 46º W), Brazil. The city has a mean annual temperature of 21.5 ºC and a mean total annual precipitation close to 1600 mm (Brazil National Weather Institute – www.inmet.gov.br). Sixteen one-year-old and 1 m tall plants were transplanted to 60 cm diameter by 50 cm high pots with soil rich in organic matter in April 2016. Ten plants had lateral branches and main stems apices pruned in order to stimulate the production of new branches of the same age, and were divided into 2 groups of five plants each: the first group was grown besides stainless steel wire meshes (7x7 cm mesh, 2.1 mm diameter wire), that served as support for stem growth, by the attachment of tendrils; the second group was grown with no support aid. A third group of 5 plants was not pruned and was also grown besides wire meshes. Pots in each group were set 1,5 m apart from each other and watered three times a week for the first year, and weekly after that. The extra non-pruned plant was grown supported with wire meshes and used for transcriptome assembling and differential gene expression analysis.

Growth Analysis

In order to assess the impact of support availability on stem growth, an analysis was conducted on newly formed branches from individuals from groups one and two, which had lateral branches and apices pruned, growing with or without the aid of support, respectively. Sixty-one branches of plants growing without support and 50 branches from plants growing with support had their length assessed with a measuring tape, the thickness of the base measured with a caliper and number of nodes counted seven times in a period of 18 months. After 30 months of cultivation, the length and base thickness of 55 and 75 first and second-order branches of plants grown with and without the aid of supports, respectively, were measured.

Impact of Support on Hydraulic Parameters and Lianescent Xylem Formation

To assess the impact of support availability on the lianescent xylem formation and on the hydraulic parameters variation along the stem (xylem amount, vessel density, equivalent vessel diameter, mean, maximum and minimum vessel diameters, hydraulic vessel diameter, specific conductivity, and proportion of vessel area), the longest branches of each individual from plants grown with and without support were analyzed. Firstly, 2 cm stem samples were collected every 50 cm beginning at the apex, avoiding nodes and any possible injuries. Fresh cross sections 10 to 25 µm thick were then produced using a sliding microtome. Sections were mounted unstained on 50 % glycerin semi-permanent slides, or double stained in 1 % Astra Blue and 1% Safranin (Bukatsch, 1972). The distance from the apex of lianescent xylem formation was measured and the most recently formed portion of xylem, comprising the 400 µm strip closest to the cambium of one interwedges region, corresponding to about one-fourth of the stem circumference, was

quantitatively analyzed in each cross section. For this purpose, images were captured using a Leica DML photomicroscope attached to a digital camera DFC 310FX, and measurements were performed using software ImageJ v1.52a (Schneider *et al.*, 2012) as described below.

The amount of xylem produced by the cambium was measured calculating the average of three straight lines from cambium to pit. Vessel density (V_d) is the number of vessels per millimeter and was calculated by counting all vessels divided by the analyzed area. Equivalent vessel diameter (D_v) of all vessels present in the analyzed regions was calculated by measuring the vessel lumen area (A) and using the formula:

$$D_v = \sqrt{\frac{4A}{\pi}}$$

From the equivalent vessel diameters, the mean (D), maximum (D_{max}) and minimum (D_{min}) vessel diameters of each sample were calculated. The hydraulic diameter (D_h), corresponding to the mean diameter that all sampled vessels would have in order to correspond to the total conductivity of the same number of vessels (n) (Tyree *et al.*, 1994, Scholz, 2013) was calculated using the formula:

$$D_h = \left(\frac{\sum_1^n {D_v}^4}{n}\right)^{\frac{1}{4}}$$

The specific conductivity (K_s) was calculated using the formula:

$$K_s = \left(\frac{\pi\rho}{128\eta}\right) \times V_d \times D_h^4$$

(Poorter *et al.*, 2010) in which the conductivity is expressed in kg m^{-1} Mpa^{-1} s^{-1}, ρ is the water density at 20°C (998.2 kg m^3), η is the water viscosity at 20°C (1,002 × 10^{-3} Pa s^{-1}), V_d is the vessel density (in m^2), and D_h is the hydraulic diameter of the vessel in meters. Yet, the proportion of vessel area (V_a) was calculated dividing the sum of vessel lumen area by total analyzed area multiplied by 100. Data analysis was performed using

generalized linear mixed-effects models of $\log_{10}$ transformed data, using individuals as random variables, in R software v.3.6.1 (R Core Team, 2014) using nlme package (Pinheiro *et al.*, 2017). Model fit and suitability of error distribution for each response variable were tested by residues analysis (Crawley 2007).

Data from basal segments of the stem, near the junctions to parental shoots, were disregarded from analysis as xylem in these portions shows a reduction in hydraulic parameters. This variation is interpreted as a hydraulic constriction that leads to water conduction segmentation of branches and leaves, and is believed to be formed in response to mechanical tensions acting near the insertion point of the branch (Zimmermann, 1983; Gartner 1995).

Xylem Anatomy Analysis

In order to characterize secondary growth establishment and self-supporting and lianescent xylem anatomy, the longest stems from the five plants that have not been pruned were sampled on May 2018. Samples were collected every 1 cm from the apex up to 5 cm, every 5 cm from 5 to 50 cm, every 10 cm from 50 cm to 1 m, and every 50 cm from 1 m up to the base, and immediately fixed in FAA 50 (10 % formalin, 5 %acetic acid, 50 % alcohol) for seven days. Samples were then dehydrated in an increasing butyl series (Johansen, 1940) and included in paraffin. Sectioning was performed from 3 to 6 µm in a rotary microtome. Alternatively, older lignified samples were rehydrated after fixation, impregnated with polyethylene glycol 1500 (PEG 1500) and transversal and longitudinal sections from 8 to 15 µm were made in a slide microtome, as described by Barbosa *et al.* (2010). Sections were mounted in Canada Balsam unstained or double stained in 1 % Astra Blue and 1% Safranin (Bukatsch, 1972). Additionally, portions of

self-supporting and lianescent xylem were dissected under stereo microscope and macerated in Franklin's solution (Berlyn & Miksche, 1976).

Self-supporting and lianescent xylem anatomies were characterized using the IAWA List of Features for Hardwood Identification (IAWA Committee, 1989) as a guide. Due to anatomical parameters variation along the stem and differences in sampled stems lengths, which ranged from 3.6 to 8.4 m, self-supporting and lianescent xylems were characterized at 4/5 of the distance to the base. In addition to the above mentioned parameters, vessel grouping index was calculated by dividing the total number of vessels by the total number of grouped vessels (Carlquist, 2001). Moreover, proportional area of fibers, axial parenchyma and rays were calculated by analyzing six 0.1 mm^2 images from random portions of the transverse section (Gerolamo & Angyalossy, 2017). For the parameters vessel element high, vessel pit diameter, fiber length, fiber wall thickness and fiber lumen area, we followed the sample size recommended by Scholz *et al.* (2013), replicating it for each xylem type in each individual. Data normality and variance homogeneity were tested using Shapiro-Wilk and Levene's tests, respectively, and average comparison were carried using Student's t-test for parametric data, and Mann-Whitney test for nonparametric data in R software v.3.6.1 (R Core Team, 2014).

Samples for Differential Expression Analysis

Tissues were collected on April 2018 by peeling the bark and gently scrapping the exposed xylem of 30 cm samples collected along the stems. Tissues were immediately frozen in liquid nitrogen and stored at -80 °C. Prior to tissue harvest each stem segment had its base cut and stored in 50 % alcohol for anatomical to determine the xylem phase, self-supporting or lianescent. Segments presenting dubious or transition anatomy, and the segment next to it, were discarded. Six pools of self-supporting and six pools of lianescent

wood forming tissue from 8 to 19 segments each were collected, forming the 12 samples used for sequencing and differential expression analysis.

RNA Extraction, Library Construction and Sequencing

Total RNA was extracted after samples lyophilization using ReliaPrepTM RNA Tissue Miniprep System (Promega Corporation) following manufacturer protocol. RNA samples were fluorometrically quantified using a Qubit (Thermo Scientific), and its integrity was confirmed by 1 % (w/v) agarose gel electrophoresis, and by a Bioanalyzer 2100 (Agilent Technologies) using the RNA 6000 Nano LabChip Kit. RNA samples with RIN ≥ 6 were considered suitable for further sequencing.

Libraries were constructed using Illumina TruSeq Stranded mRNA Sample Prep LT Protocol (Illumina), and paired-end sequences of 100 bp were generated on a HiSeq2500 platform, using a HiSeq Flow Cell v4 with HiSeq SBS Kit v4 (Illumina) at Centro de Genômica Funcional Aplicada a Agropecuária e Agroenergia, ESALQ, USP, Piracicaba, São Paulo, Brazil.

Sequence Analysis

Adaptors and low-quality sequences, below 23 and 30 Phred quality parameter for maximum average error and maximum error at end, respectively, were trimmed using SeqyClean v.1.9.10 (Zhbanikov *et al*., 2017). Only high-quality paired end sequences were used for further analysis. Contaminant sequences were removed using HISAT2 v2.0.5 (Kim *et al*., 2015). For contaminant identification, a contaminant bank was built containing sequences of Bacteria, Nematoda, Oomycetes and Platyhelminthes with assembled complete genome, chromosome or scaffold from reference or representative genomes (RefSeq category). Data were downloaded on December 2017, using NCBI

Entrez Direct E-utilities v6.60 (Kans, 2017). In addition, small and large rRNA subunit sequences were downloaded from Silva database version 128 (Quast *et al.*, 2012). Quality-filtered reads were aligned against contaminant bank database using the HISAT2 flag "un-conc" in order to recover paired-end sequences that fail to align concordantly to contaminants. *De novo* transcriptome assembling was then generated using Trinity v.2.8.3 (Haas *et al*., 2013) with default parameters. The longest isoforms were extracted using a Perl script.

The *de novo* assembled transcriptome was annotated against Viridiplantae SwissProt database (www.uniprot.org) (downloaded on September 18, 2019) by BLASTX program, of BLAST suite (BLAST® Command Line Applications User Manual), with 1e-5 e-value threshold. Annotated assemblies had their GeneOntology (GO) terms retrieved with the tool "Retrieve/ID mapping" in the UniProt website (www.uniprot.org), and parental terms were recovered using BLAST2GO "Combined Graph" tool (Conesa *et al*., 2005).

Further, *B. magnifica* cambium and differentiating xylem transcriptome was compared against the counterpart from wood forming tissues from the model species *Populus* (*P.* × *euramericana*) and *Eucalyptus grandis* annotated by Zinkgraf *et al*. (2017), over the data generated by Xu *et al*. (2014). *A. thaliana* orthologs of each expressed gene from the two model species retrieved by the authors were used to recover the associated GO terms using the UniProt website. For transcriptome comparison purpose, we selected the Biological Process GOs associated with at least 10 % of the GO term-associated transcripts by BLAST2GO "Combined Graph" tool, for all three species. The heat map created to visualize the functional comparison between *B. magnifica*, *Populus* and *Eucalyptus* was produced using the online tool Morpheus (Broad Institute, accessed at https://software.broadinstitute.org/morpheus/).

For differential expression analysis, the 12 RNA-Seq samples were mapped over the GO term-associated transcripts using Salmon v.0.11.3 (Patro *et al*., 2017). The transcript abundances were then used to identify the differentially expressed genes (DEGs) between self-supporting and lianescent-phases. The significance of differences was assessed with the package edgeR v.3.26.8 (Robinson *et al*., 2010), from Bioconductor v.3.9 software (Huber *et al*., 2015). For this purpose, we normalized the 12 libraries with the TMM method (Robinson & Oshlack, 2010) using the calcNormFactors() function, while common dispersions were calculated with the estimateCommonDisp() function (Robinson & Smyth, 2008). Threshold adopted for significance assessing was $p < 0.05$, false discovery rate (FDR) < 0.05 and log2 fold change > 2. GO functional enrichment analysis of DEGs was performed by Fisher exact test (FDR < 0.05).

Results

Growth Analysis

Plants grown with or without support, which had lateral branches and apices of main stems pruned, had their developing shoots measured for 18 months, from April 2016 to September 2018. In total 50 branches of plants cultivated with the aid of supports and 61 branches of plants cultivated without the aid of supports were scored during the first 14 month of growth. The length and number of nodes of the branches from plants grown with and without support aid was the same until December 2016, when they had 62 cm (± 14.3) and presented 11 (± 1.1) nodes (Fig. 2a,b), when the first leaves with functional tendrils began to develop. In fact, until the ninth node, the leaves could be either simple (commonly just in the first node), have three expanded leaflets, fail to produce the third leaflet/tendril, or could produce senescent tendrils. After 10 months of growth, in February 2017, branches of plants cultivated with support were almost twice as long than

those from unsupported plants (175 ± 27 cm and 89 ± 24 long, respectively), while the number of nodes was still the same, indicating that the difference in length was due to internode elongation. In September 2017 (18 months of growth), both length (340 ± 37 cm and 114 ± 36 long, respectively) and number of nodes (28 ± 2 and 19 ± 2, respectively) were significantly larger in the branches of plants cultivated with the aid of support. The thickness of the shoot bases, in turn, did not vary between plants cultivated with and without support during the first 18 months of growth (Fig. 2c).

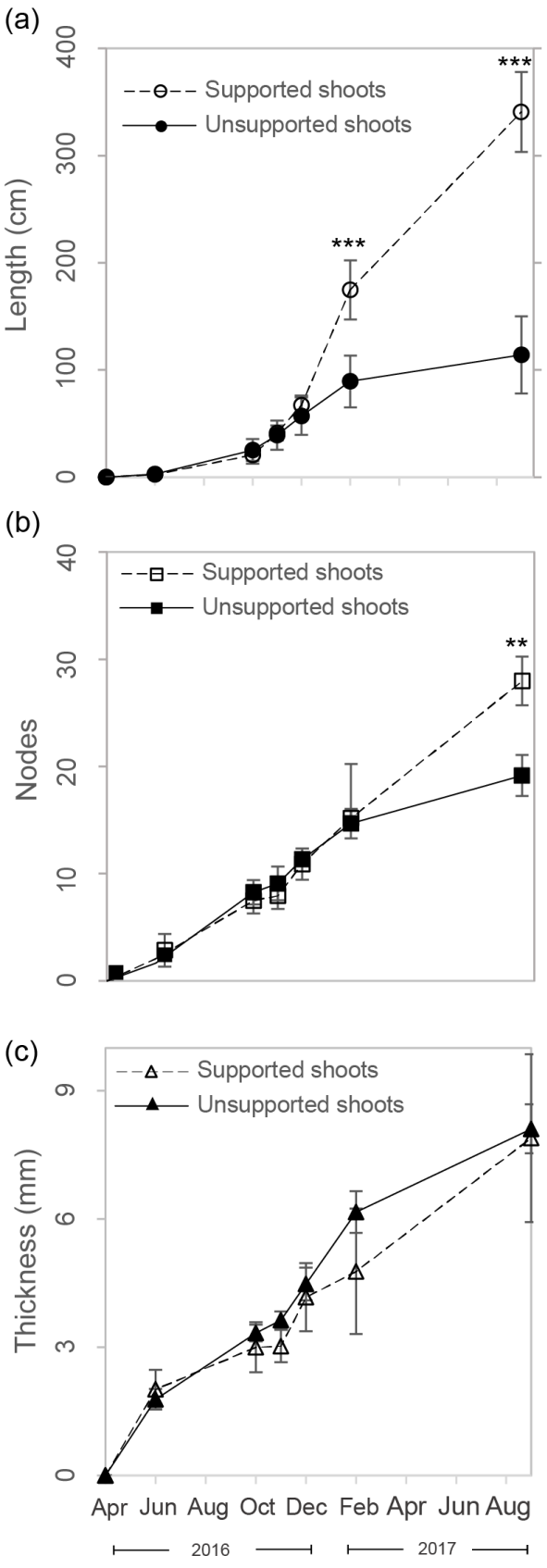

At the end of thirtieth months of growth, we compared length and thickness at the base of branches of first and second order from plants grown with and without the aid of supports. First and second-order branches were

Fig. 2 *B. magnifica* new branches growth in the first 18 months (from April 2016 to September 2017). Error bars represent ±SD from 50 branches grown with support and from 61 branches grown without support. Asterisks denote statistical significance: ***, $p < 0.001$; **, $p < 0.01$.

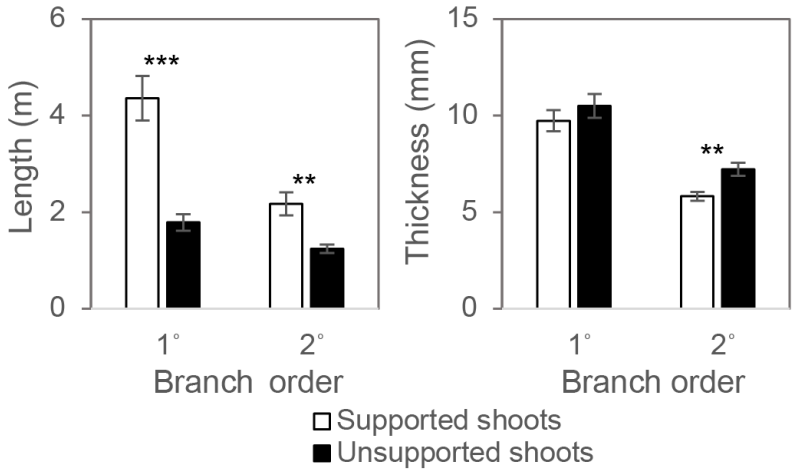

Fig. 3 Difference in first and second order branches growth in plants grown with and without supports after 30 months of cultivation (from April 2016 to October 2018). Error bars represent ± SE from 21 1st order branches grown with support; 34 1st order branches grown without support; 38 2nd order branches grown with support; and 37 2nd order branches grown without support. Asterisks denote statistical significance: ***, $p < 0.001$; **, $p < 0.01$.

longer in plants grown with the aid of support, averaging 436 cm (± 211) and 217 cm (± 148) respectively, while their counterparts from plants grown without support had 179 cm (± 78) and 124 cm (± 53), respectively. Shoot base thickness, on the other hand, did not differ in first-order branches and was smaller in second-order branches in plants grown with supports, with an average thickness of 7.2 mm (± 2) and 5.8 mm (± 1.4), respectively (Fig. 3).

All together these data clearly exposed that the presence of support increases length growth in the liana *B. magnifica* and decreases the growth in thickness.

Impact of Support on Hydraulic Parameters and Lianescent Xylem Formation

Xylem structure along the stem of the longest branch of each plant grown with and without the aid of supports was then analyzed. The subset of analyzed supported branches had 6.6 m (± 1.6) in length and 10.4 mm (± 3.6) in diameter at the stem base, while the

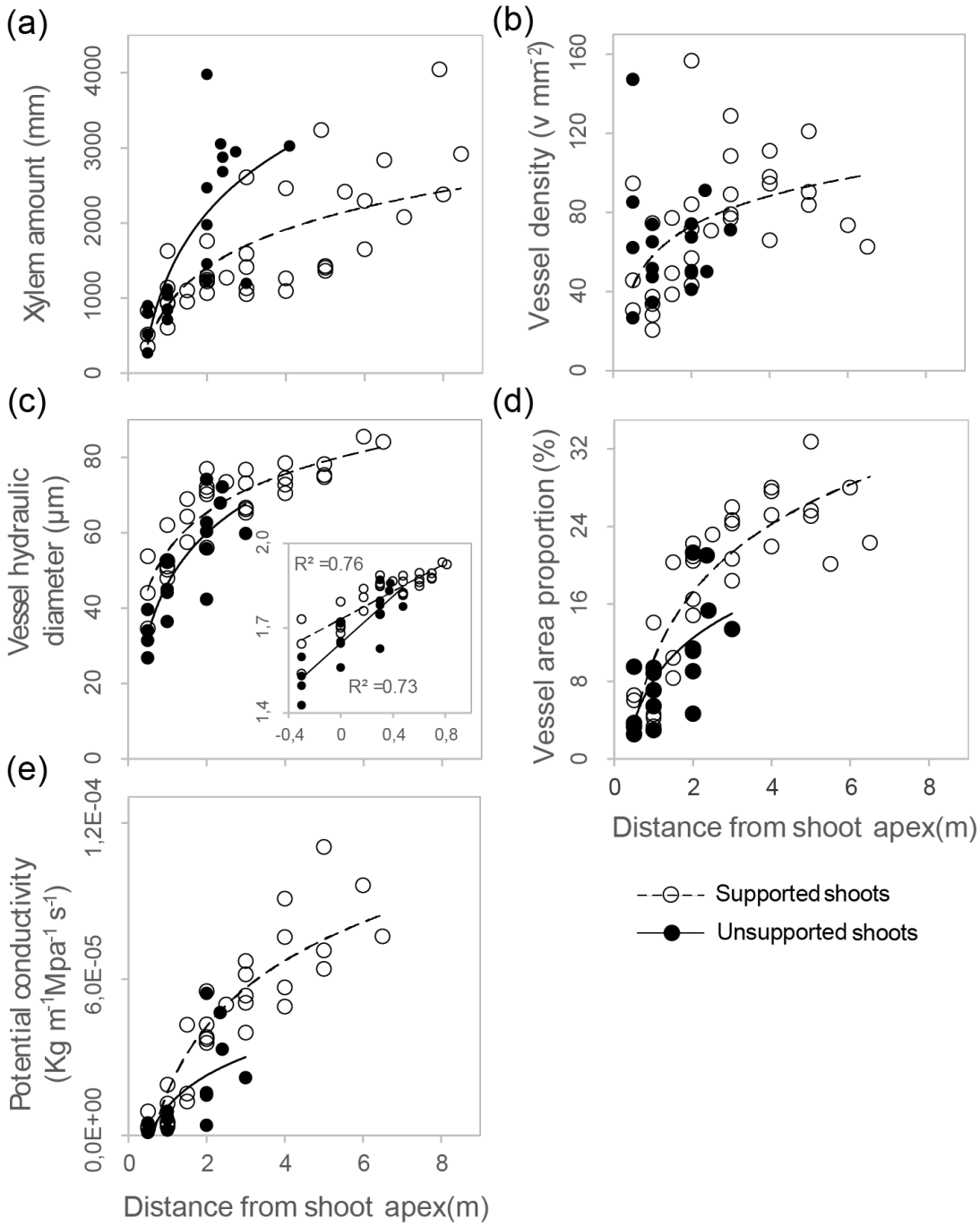

Fig. 4 Variation of hydraulic parameters along the stems grown with and without support. Lines indicate significant fit of linear mixed-effects models of $\log_{10}$ transformed data using individuals as random variables ($p < 0.001$). Fit of linear regression of $\log_{10}$ vessel hydraulic diameter and $\log_{10}$ distance from apex showed a higher slope, of 0.41, for branches grown without supports ($R^2 = 0.73$), and a slope of 0.24 ($R^2 = 0.76$) for branches grown with support ((c) inset), indicating a higher variation of this parameters along the length of those branches

subset of unsupported branches had 2,7 m (±0,8) in length and 9,4 mm (±0,8) in diameter

at the stem base.

Xylem production was higher in the shorter unsupported branches at the same distances from the apex, in comparison to the longer branches grown with the aid of support (Fig. 4a, greater slope of the log transformed data regression, Supporting Information Fig. S1, and Table S1). Vessel hydraulic diameter, vessel area proportion, and specific conductivity increased towards the base of the stem in both groups, while only plants grown with support showed a significant correlation between vessel density and distance from the apex (Fig 4). Density of vessels varied from 20.6 to 156 vessels per mm in plants grown with support, increasing toward the base, and from 26.7 to 147.1 in plants grown without support (Fig. 4b), although, as mentioned above, it does not significantly correlate with distance from the apex. Vessel hydraulic diameter (D_h) was higher at more basal parts of the stem in plants grown with supports, varying from 44 µm near the apex to 84 µm 6.5 m below, while in plants grown without supports D_h varied from 31 µm near the apex to 60 µm 3 m below (Fig. 4c). However, plants grown without supports showed a higher variation in vessel hydraulic diameter (slope = 0.41, $R^2 = 0.73$, data log-transformed) along the stem than plants grown with support (slope = 0.24, $R^2 = 0.76$, data log-transformed), although the unsupported plants showed a limited length growth for this parameter.

Vessel area proportion was also higher in basal parts of plants grown with supports, varying from 3 % to more than 30%, while in plants grown without supports these values varied between 3 % and 21 %, but most samples showed values less than 15 % (Fig. 4d). Nevertheless, the variation along the stem, as showed by the slope of the log transformed data regression, was similar between the two groups (Supporting Information Fig. S1). Specific conductivity followed the variation of hydraulic diameter, and was higher in plants grown with supports, but its variation along stem length was higher in plants grown

without support (Fig. 4e, Supporting Information Fig. S1). The range of specific conductivity varied from 2.8×10^{-6} to 9.6×10^{-5} Kg m^{-1} Mpa^{-1} s^{-1} along stems grown with supports, and from 1.1×10^{-6} to 5.5×10^{-6} Kg m^{-1} Mpa^{-1} s^{-1} along stems grown without supports.

The most striking change along the stem, however, was the production of the lianescent xylem, which occurred in all plants grown with supports and in a single plant grown without support. Beginning of lianescent xylem production was initially recognized by the concomitant production of several large vessels along the circumference of the cambium (Fig. 6b), which occurred between 1.5 m and 2 m from the stem apex in all plants showing this type of xylem. To further understand the anatomical changes along the stem that culminate in the production of lianescent xylem, we have characterized the anatomy of *B. magnifica* xylem since its primary development in mature stems of group 3 of plants, which did not had lateral branches or apexes pruned, with emphasis on the differences between the self-supporting and lianescent phases.

In summary, our results show that the presence of support changes how hydraulic parameters vary along the stem, increasing vessel area proportion and specific conductivity, while reduces xylem production and vessel hydraulic diameter, and triggers lianescent xylem formation.

Xylem Development Analysis

The vascular system in primary structure near the stem apex is composed of a continuous procambium cylinder (Fig. 5a), that forms collateral vascular bundles and numerous phloem strands between the collateral bundles (Fig. 5b, black and white arrows respectively) between the vascular bundles. The installation of a continuous cambium occurs around 5 cm below stem apex, producing secondary xylem that is composed

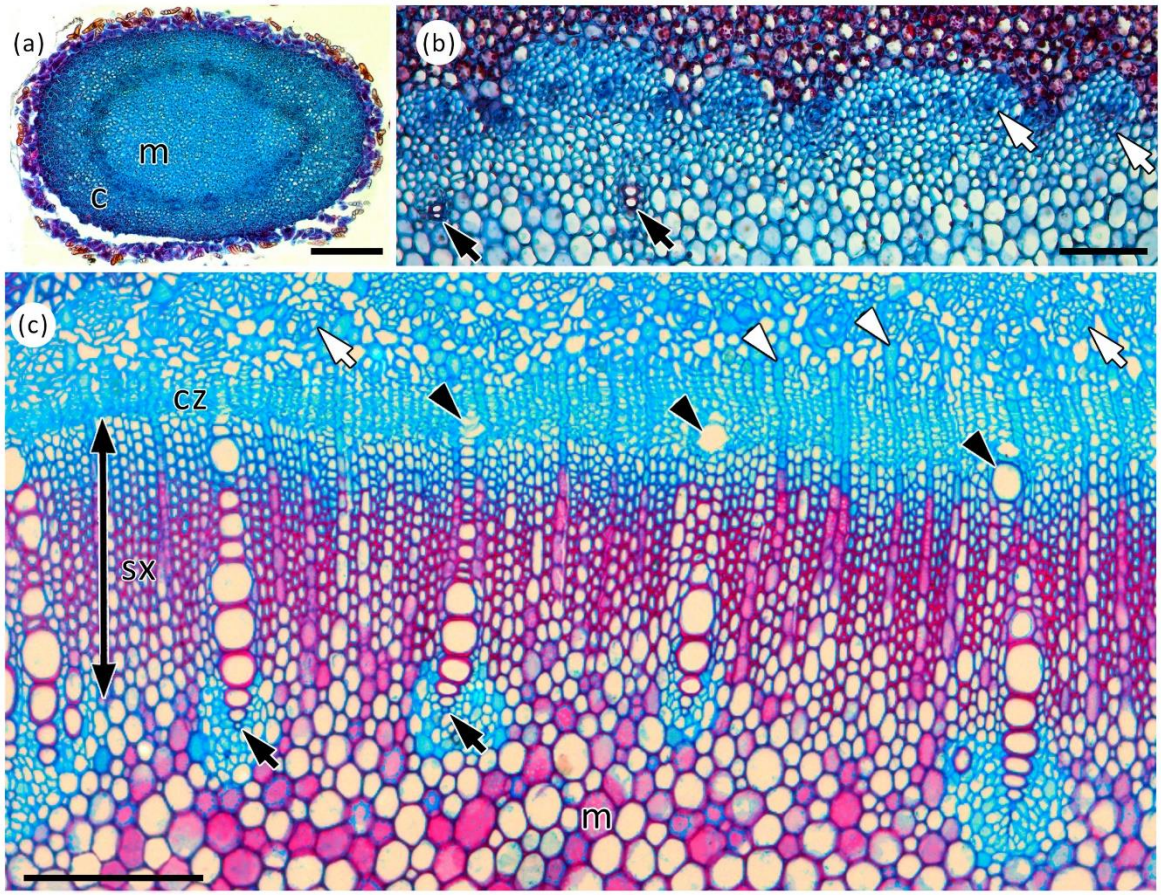

Fig. 5 Stem vascular system in primary structure and establishment of secondary growth in *B. magnifica*. (a) Vascular system composed of a cylinder of denser celled procambium, delimiting cortical (**c**) and medullary (**m**) regions near the stem apex. (b) Vascular system in primary structure, composed of collateral bundles (black arrows point to the bundles protoxylem pole) and phloem cords (white arrows). (c) Secondary xylem (**sx**) production starts with the formation self-supporting phase xylem. In this phase new vessels are produced only in front of protoxylem poles (black arrows), forming a radial arrangement of vessels. From left to right we can see three stages of vessel differentiation (black arrow heads): early cell growth, late cell growth, and secondary cell wall deposition and beginning of lignification. Production of secondary phloem is delayed in comparison to xylem production. Phloem is composed mainly by primary phloem cords (white arrows) and phew cell layers of secondary phloem (white arrow heads point to the first formed phloem ray cells). Scale bars: (a) and (b): 200 µm; (c) 75 µm.

mainly by a matrix of septate fibers and rays, while vessels, and scanty associated axial parenchyma, are produced only in front of the protoxylem poles (Fig 5c). This restriction on vessel production is maintained throughout the self-supporting phase (Figs. 5c, 6a, b, and c), conferring a radial arrangement to the vessels, opposite to the protoxylem poles.

The rays in self-supporting phase xylem are uniseriate and composed of upright and square cells (Fig. 6d, left portion).

The onset of lianescent xylem formation is marked by the concomitant production of several large vessels throughout the width of the cambium (Fig. 6b and c), as mentioned above. These large vessels may be solitary or associated with small vessels, what characterizes the vessel dimorphism common to all lianas, and forms a bimodal distribution of vessel diameter classes in *B. magnifica*. Vessel diameter distribution shows that the increase in mean, hydraulic and maximum vessel diameters are due to a new class of vessels, with a peak in 111µm (Fig. 7). Fibers are also septate in lianescent xylems, but ray width and ray cell composition change. Rays are uni to biseriate, and transversal divisions of upright ray initials at the beginning of this phase produce cells that are predominantly square and procumbent square (as seen in Fig. 6d, right portion).

This analysis revealed qualitative changes associated with lianescent xylem formation, as the end of the vessel production restriction in front of protoxylem poles, production of large vessels and procumbent ray cells.

Self-Supporting and Lianescent Xylem Characterization

To further understand the differences between self-supporting and lianescent xylem, we quantitatively evaluate the xylem of both phases (Table 1). The most obvious difference refers to vessel relative area, that in the lianescent xylem represents 35.9 %, compared to only 5.7 % in the self-supporting phase, an increase of more than five times (Table 1). This increase occurs at the expense of fiber relative area, which decreases from 81.6 % in self-supporting, to 54.7 % in lianescent xylem, and radial parenchyma, which decreases from 12 % to 7.7 %. The axial parenchyma, extremely rare and associated with the

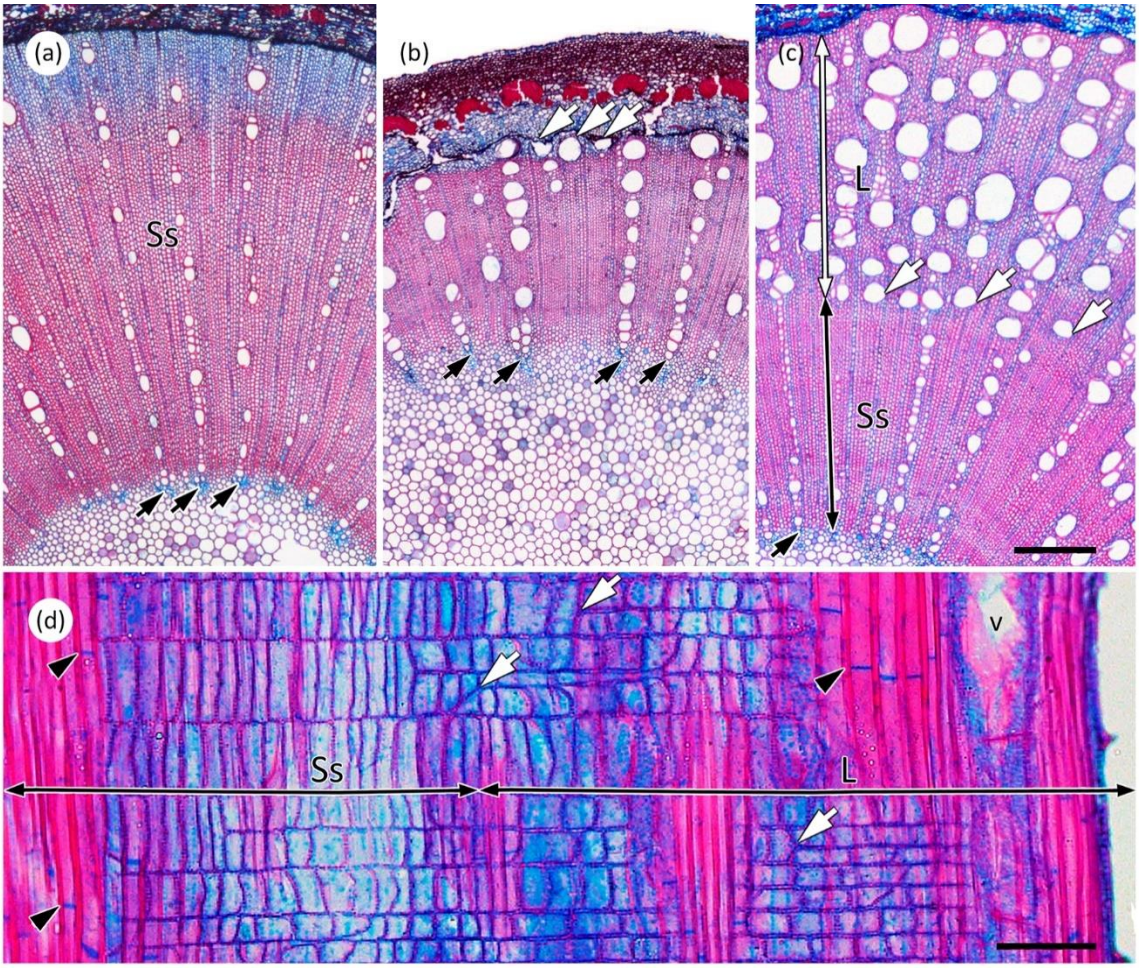

Fig. 6 *B. magnifica* self-supporting and lianescent xylem. (a), (b) and (c) Stem cross section. (a) Self-supporting xylem (**Ss**) is characterized by small vessels radially arranged formed only opposite to protoxylem poles (black arrows), and a high proportion of fibers. (b) Onset of lianescent xylem formation is marked by the concomitant production of large vessels (white arrows) alternating with protoxylem poles (black arrows) and radial files of vessels. (c) Older portion of the same stem as in (b) showing a larger amount of lianescent xylem (**L**, white double headed arrow) formed to the outside of the first formed self-supporting xylem (**Ss**, black double headed arrow). The first large vessels (white arrows) formed alternate to the radial files of vessels of self-supporting xylem mark the onset of lianescent xylem, that is characterized by large proportion of vessel area and large vessels, that may be solitary or associated with small vessels. (d) Radial view of the transition from self-supporting xylem (**Ss**, to the left of the figure) to lianescent xylem (**L**, to the right of the figure). Ray composition changes from upright cells in **Ss** to mainly square and procumbent cells in **L** due to transverse divisions of ray initials, which products are seen (marked by white arrows); while vessels (**v**) are more frequently found in **L**, due to their larger size and arrangement. Septate fibers (arrow heads point to the septa), on the other hand, are found in the xylem of both phases. Scale bars: (a), (b) and (c): 350 µm; (d): 100 µm.

vessels, increases from 0.6 % to 1.7 %, a smaller increase then would be expected if it accompanied the increment of vessels area.

Increase of vessel area is due to the increase in vessel size, and not to the vessel density. The mean, maximum and hydraulic vessel diameters are 73 %, 92 % and 103 %, larger in the lianescent xylem in comparison to the self-supporting xylem, respectively, while vessel density and minimum vessel diameter does not vary between the two phases, as is also the case of vessel element length (Table 1). The increase of vessel diameter in lianescent xylem results in an increase of more than 20 times of the specific conductivity, from 4.52×10^{-6} in self-supporting xylem, to 106.98×10^{-6} kg m^{-1} Mpa^{-1} s^{-1} in lianescent xylem. Pit diameter was another characteristic related to hydraulic conductivity that increased, from 4.28 µm in self-supporting to 4.95 µm in lianescent xylem. In the same way, vessel grouping index, that shows the average number of vessels per vessel groupings, was higher in lianescent xylem, with 3.6 vessels, while self-supporting xylem showed 2.4 vessels per vessel grouping. The fibers of both xylem phases are septate, remaining alive at maturity. However, fibers are wider, shorter, and have thicker cell walls in the lianescent xylem, in comparison to the self-supporting xylem (Table 1).

In conclusion, several anatomical traits are quantitatively diverse in lianescent xylem, notably specific conductivity, vessel relative area and hydraulic vessel diameter.

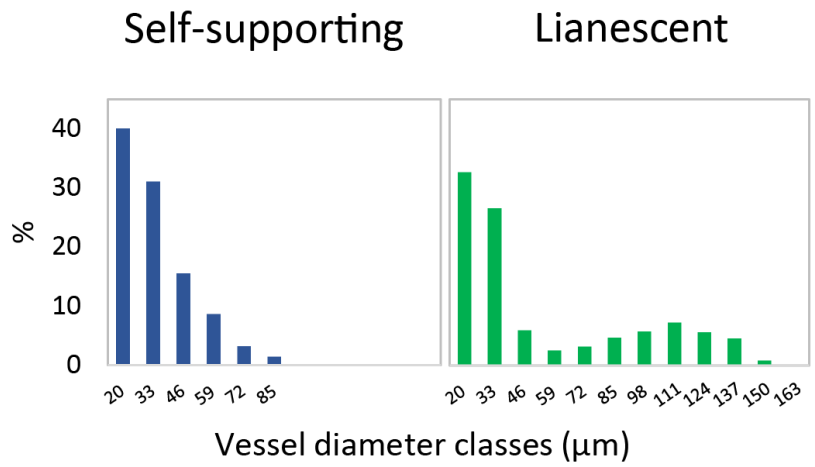

Fig. 7 Self-supporting and lianescent xylem vessel diameter classes distribution.

B. Magnifica Cambium Transcriptome Assembling

In order to understand the transcriptional regulation responsible for the formation of the two distinct xylems characterized above, we conducted an RNA-Seq analysis of the active cambium and differentiating tissues of both phases. Six biological samples of each phase, corresponding to pools of stem segments, were sequenced, producing 512 millions of 100 bp, paired end reads (40 GB, Supporting Information Table S2a). *De novo* assembling was performed using the Trinity package after trimming adaptors and low-quality sequences and cleaning contaminant reads, yielding 133,883 assemblies, from which 54,207 longest isoforms were recovered (Fig. 8, Supporting Information Table S2a).

Functional Annotation

The 54,207 longest isoforms were annotated against Viridiplantae sequences available at SwissProt database using BLASTX. A total of 20,548 transcripts were recovered with positive matches and; 20,428 of those were found to be associated to Gene Ontology terms (GO), which we used for further analysis (Supporting Information Table S2b). Out of the 7,198 unique terms identified, 3,738, 2,714, and 746 were related to biological processes, molecular functions and cellular components, respectively. We then compared *B. magnifica* functional annotation with those previously reported for the woody forming tissues from the model species *Eucalyptus grandis* and *Populus* × *euramericana* (Zinkgraf *et al.*, 2017). We found a higher number of transcripts with associated GO terms in the cambium of *B. magnifica* (20,428; Supporting Information Table S3) than in the other two species, 15,127 and 14,186 for *E. grandis* and *P.* × *euramericana*, respectively. This difference could be explained because *B. magnifica* was annotated against Viridiplantae database, while *E. grandis* and *P.* × *euramericana* were annotated using

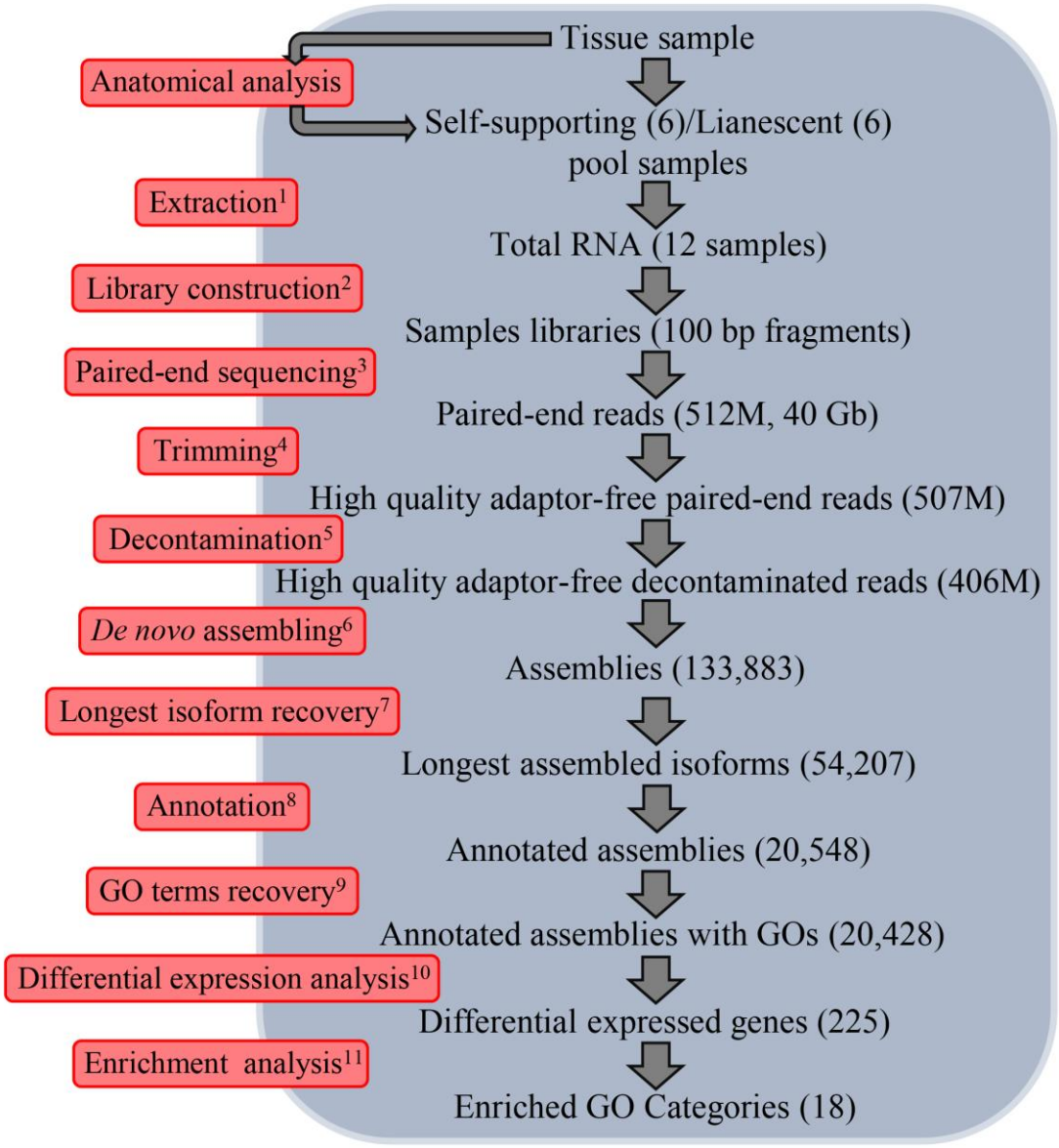

Fig. 8 RNA-seq experiment workflow. 1 - total RNA was extracted using ReliaPrepTM RNA Tissue Miniprep System (Promega Corporation) following manufacturer protocol; 2 - libraries for sequencing were constructed using Illumina TruSeq Stranded mRNA Sample Prep LT Protocol (Illumina); 3 - RNA libraries were multiplexed and sequenced on a HiSeq2500 system, using a HiSeq Flow Cell v4 with HiSeq SBS Kit v4 (Illumina); 4 - adaptors and low quality sequences were trimmed using SeqyClean v.1.9.10 (Zhbanikov *et al.*, 2017); 5 - decontamination was performed using HISAT2 v2.0.5 (Kim *et al.*, 2015) against a contaminant bank (see Material and Methods for contaminant bank details); 6 - de novo transcriptome assembling was generated using Trinity v.2.8.3 (Haas *et al.*, 2013); 7 – longest transcripts isoforms were recovered using a Perl script; 8 - autommatic annotation was performed using BLASTX (BLAST® Command Line (*continues on the next page*)

only *A. thaliana* data (Zinkgraf *et al.*, 2017). Additionally, while *B. magnifica* transcriptome was *de novo* assembled, the model species counterparts were whole

genome-supported and, thus the number of transcripts might be more accurate. However, we might not discard the possibility that the higher number of transcripts in *B. magnifica* reflects a more complex transcriptome due to the contrasting characteristics of lianescent and self-supporting xylems in this species. To further understand functional similarities among the cambium of the three species, we compared those Biological Processes GO terms associated with at least 10 % of the transcripts. Fifty-three, 54 and 159 Biological Processes GOs were identified for *E. grandis*, *P.* × *euramericana* and *B. magnifica*, respectively. All *E. grandis* and *P.* × *euramericana* GOs were shared with *B. magnifica* and showed highly similar relative number of associated transcripts (Fig. 9a). Interestingly, we also found 105 Biological Processes exclusively represented in *B. magnifica* (Fig. 9b), that might encompass transcripts with *B. magnifica* exclusive functions.

Differential Expression Analysis

In order to identify differential expressed genes (DEGs) between self-supporting and lianescent cambium, we firstly evaluated the quality of the twelve biological replicates. A multidimensional scaling (MDS) was performed and showed that both set of samples grouped together demonstrating their suitability to further analysis (Figure S2).

By applying a significance cut off of $p < 0.05$, false discovery rate (FDR) < 0.05 and $-2 > \text{logFC} > 2$ (Fig. 10a), 140 (Supporting Information Table S4a) and 85 (Supporting Information Table S4c) assembled transcripts were identified as up-regulated

Fig. 8 (*cont.*) … Applications User Manual) (against SwissProt Viridiplatae database (downloaded on Spetember 18 2019); 9 - GO terms were recovered with the "Retrieve/ID mapping" tool in the UniProt website (www.uniprot.org); 10 – reads were quantified using Salmon v.0.11.3 (Patro *et al.*, 2017), and abundances were used to estimate DEGs using the package edgeR v.3.26.8 (Robinson *et al.*, 2010), from Bioconductor v.3.9 software (Huber *et al.*, 2015); 11 - Enrichment analysis was performed applying a Fisher exact test (FDR < 0.05).

in self-supporting and lianescent cambium, respectively. An enrichment analysis was performed by Fisher test ($p < 0,05$) for the three main functional categories: *biological process*, *molecular function* and *cellular component*. In self-supporting wood forming tissue, the enriched categories could be clustered into three groups associated with: cell wall (*cell wall organization or biogenesis*, GO:0071554; *plant-type cell wall organization or biogenesis*, GO:0071669; *extracellular region*, GO:0005576; *anchored component of membrane*, GO:0031225 and; *external side of plasma membrane*, GO:0009897), all of them overrepresented; transcriptional regulation (*nucleus*, GO:0005634; *nuclear part*, GO:0044428; *organic cyclic compound binding*, GO:0097159; *heterocyclic compound binding*, GO:1901363; *nucleoside phosphate binding*, GO:1901265; *nucleotide binding*, GO:0000166), all underrepresented; and protein metabolism (*protein metabolic process*, GO:0019538; *nitrogen compound metabolic process*, GO:0006807), also showing all underrepresented terms (Supporting Information Table S4b). In lianescent cambium the category *response to stimulus* (GO:0050896), which encompasses *response to organic substance* (GO:0010033), *response to hormone* (GO:0009725) and *response to endogenous stimulus* (GO:0009719), was highly enriched, suggesting the role of hormone signaling in xylem differentiation including cell wall deposition and cell death triggering. Additionally, the molecular function *L-glutamine transmembrane transporter activity* (GO:0015186) showed to be enriched as well (Supporting Information Table S4d), both categories overrepresented.

To better understand the gene functions that determined the differences between self-supporting and lianescent xylem differentiation, we performed a hand-curated comprehensive annotation of all DEGs (column J, Supporting Information Table S4a,c). It is evident that self-supporting phase xylem is a more homogeneous tissue due to the higher proportion of fibers and radially arranged small vessel elements. In contrast, the

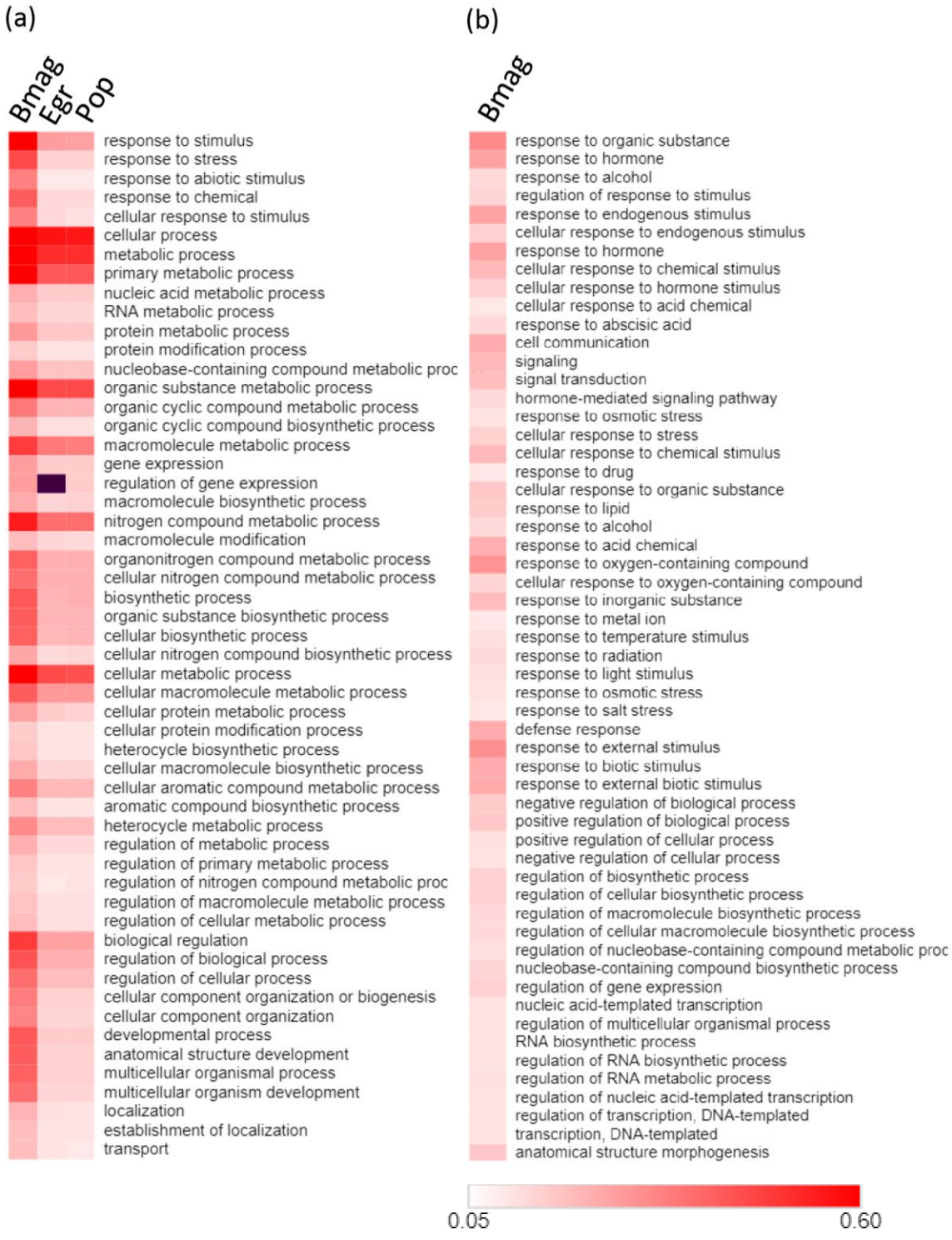

Fig.9 (*The figure continues on the next page*) Comparative functional annotation of cambial transcriptomes from *B. magnifica* and the model species *Eucalyptus grandis* and *Populus* × *euramericana*. Color scale shows the relative number of transcripts associated with Biological Process-related GOs. GOs with at least 10% of associated transcripts out of the total of each transcriptome were included in the heat map. Black cell: term not present.

(b) cont.

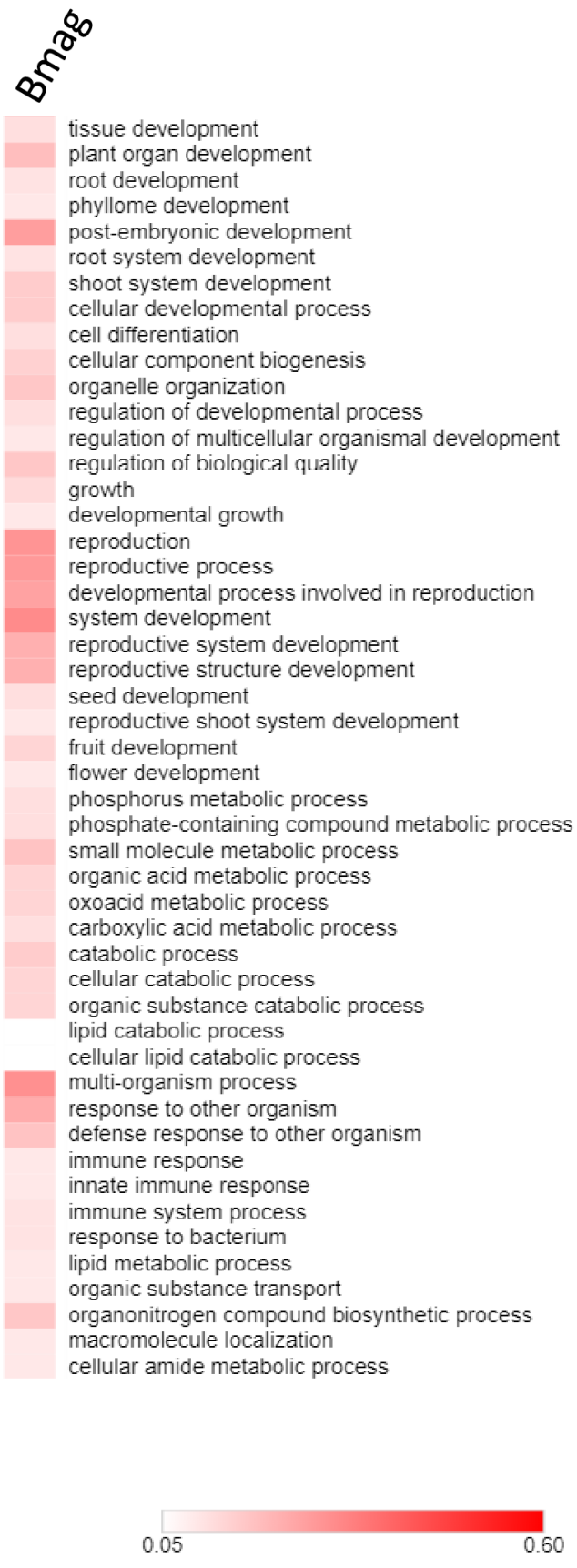

lianescent xylem shows a lesser proportion of fibers and a higher proportion of vessels, which are formed throughout stem circumference and are of two distinct size classes. Consequently, it is expected that a wider spectrum of genes would be needed in the later to determine the higher functional diversity. In this sense, the DEGs in lianescent xylem displayed a higher proportion of transcriptional factors (17 %) and hormone responsive genes (20 %) compared to the self-supporting counterparts, 11 % and 3%, respectively. Additionally, 21 % of the DEGs identified in the lianescent tissue correspond to genes involved in defense/cell death mechanisms associated to the vessel elements formation, in contrast, only 12 % of the DEGs belong to this category in self-supporting sample, reflecting the fact that the fibers in

both types of wood are septate, remaining alive at maturity. In line with the higher number of cells per area and the conspicuous cell wall and lignin deposition in self-supporting xylem, 10 % and 29 % of the DEGs are associated to cell division and cell wall, contrasting with only 4 % and 13 % in lianescent tissue, respectively (Fig. 10b).

Next, we investigated whether some of the DEGs between lianescent and self-supporting xylem were associated with *B. magnifica* exclusive processes, in comparison to *E. grandis* and *P.* × *euramericana* transcriptomes. For this purpose, we selected those DEGs associated with the 105 *B. magnifica* exclusive Biological Processes GOs (Fig. 10b). From those, we excluded the transcripts that were also associated with the 53 shared Biological Processes GOs. Out of the 85 and 140 DEGs for lianescent and self-supporting xylem, this analysis resulted in 45 and 50 transcripts only associated with *B. magnifica* exclusive GOs, respectively (Fig. 10b, Supporting Information Table S5). The most representative categories among these DEGs were transcription factor, hormone response and defense/cell death in transcripts up-regulated in the lianescent xylem, displayed by 12.9 %, 11.8 % and 10.6 % of all DEGs of this tissue, respectively. Amidst up-regulated DEGs in the self-supporting forming tissue, cell wall was the most represented category, present in 12.1 % of the DEGs. In fact, the greater part of the DEGs involved in transcription factor, cell growth/differentiation, cell wall and hormone response in the lianescent xylem forming tissue presented only Biological Processes exclusive to *B. magnifica*, as well as defense/cell death in the self-supporting tissue (Fig. 10b).

Concluding, the differential expression analysis unraveled distinct functional profiles in the repertory of transcribed genes that result in the unique morpho-anatomical and functional features described above.

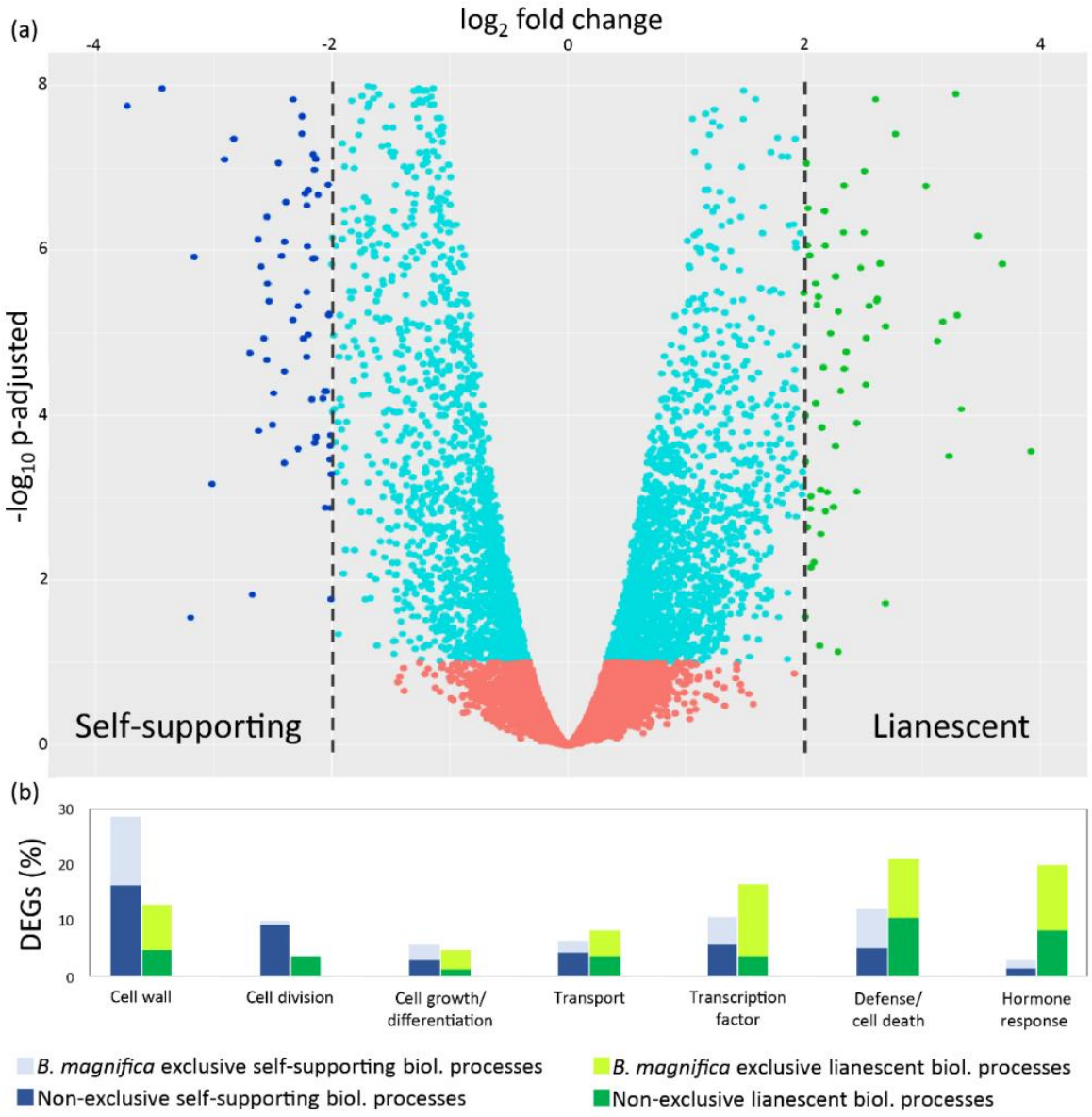

Fig. 10 Differential exprension between self-supporting and lianescent xylem forming tissues and hand curated categories enrichment analysis. (a) Volcano plot showing transcript expression significance versus fold-change of 240,428 annotated transcripts which were associated with GO terms. A total of 225 differentially expressed genes (DEGs) were recovered using a cutoff of $p < 0.05$ and log2 fold change > 2: 140 up-regulated in self-supporting xylem forming tissue (blue points) and 85 up-regulated in lianescent xylem forming tissue (green points). (b) Seven most represented categories of hand curated comprehensive annotation of the 225 DEGs. Darker colours (base of columns) indicate transcripts that share GO terms with the model species E. grandis or P. × euroamericana; clearer colours (top of columns) indicate transcripts that do not share any GO terms with those species. In total 183 (81%) DEGs were annotated in these categories.

Discussion

In the present work, we characterize in detail how the presence of support changes stem growth and xylem differentiation in the liana species *Bignonia magnifica*. We have demonstrated that the presence of support decreases the formation of xylem of shoots in *B. magnifica*, whereas stimulates growth in length, changes the variation of anatomical parameters along the stem, increases specific conductivity, and promotes the formation of lianescent xylem, to the detriment of self-supporting phase xylem. We have also described qualitatively and quantitatively the xylem of both phases and showed that the more complex anatomy in lianescent phase is the result from a more complex transcriptional regulation, involving transcriptional factors and hormone responsive genes.

The Presence of Support Differentially Impacts Stem Growth in Length and Thickness, Consequently Influencing Hydraulic Parameters Variation Along the Stem

Together with xylem characteristics, as higher amount of fibers and small vessels, the absence of tendrils in the first formed leaves of a shoot, or its senescence, can be seen as a sign of the self-supporting nature of young stems. Increase in length growth and leaf production in the presence of supports could only be seen after the production of the 11th node, when functional tendrils were first formed and attached to supports. The increase in growth in the presence of support in combination with a well-marked self-supporting phase, may represent an ecological strategy for colonization of the canopy (Caballé, 1993).

The presence of supports decreased thickness growth and changed the variation of hydraulic parameters along the stem. The sequential anatomic analysis allowed us to

observe that the variation of hydraulic parameters along the stem does not follow the abrupt change observed in xylem anatomy in the transverse section. Rather, the observed changes were on the slope of hydraulic traits regression curves, with variation rates diverging between plants grown with or without supports. Although plants grown without support did not formed the lianescent xylem, the variation in vessel hydraulic diameter (D_h) along their stem length (L) was $D_h = L^{0.41}$, while the value for plants grown with supports, which did formed the lianescent xylem, was $D_h = L^{0.24}$. This last value agrees with the expected by the hydraulic optimality hypothesis (Petit & Anfodillo, 2011) and with that found by Olson *et al.* (2014), of $L^{0.22}$, and proposed to be universal among the Angiosperms. This is because D_h variation with exponents close to 0.2 leads to the conservation of hydraulic conductivity resistance regardless of plant length. Variation with exponents higher than 0.2, on the other hand, would lead to very large vessels for a given stem length and an exceedingly thick stem, without reduction in conductivity resistance and with a greater embolism risk. This could indicate the dependence of support for normal development of the xylem in *B. magnifica,* or yet, the existence of a more complex pattern of vessel diameter variation along Angiosperm stems, modulated by endogenous and environmental cues (Hacke *et al.*, 2017).

The decrease of vessel density with the increase in vessel diameter is a universal trend among woody plants (Baas *et al.*, 1986) that reflects "the compromises between maximizing the area for conduction versus mechanical support" (Sperry *et al.*, 2008). The concomitant increase of vessel density and vessel diameter shows the conductivity bias over the support function of *B. magnifica* stems grown with supports.

Lianescent Xylem Differs Quantitatively and Qualitatively from Self-Supporting Xylem

The most evident difference between plants grown with and without supports was the change in production from self-supporting xylem to lianescent xylem. Self-supporting xylem, also referred as inner system (Ewers & Fisher, 1989), inner xylem (Ewers *et al.*, 1991; Rowe & Speck, 1996), *bois axial* or *bois dense* (Obaton, 1960) is composed by a larger proportion of fibers and smaller vessels, a characteristic shared with many other lianas (Schenck, 1893; Carlquist, 1991; Caballé, 1993). An unexpected trait found in the self-supporting xylem was the restriction of vessels, found almost exclusively opposite to protoxylem poles. The production of vessels only in this specific position can be seen as a restraint of vessel formation signals to the cambial initials occupying this location. Obaton (1960) cites the presence of radially arranged vessels in self-supporting xylem in some African liana species but did not mentioned the restriction of vessel formation as found in *B. magnifica* stems. Whether the pattern of vessel production opposite to protoxylem poles is unique to *B. magnifica* or is a feature of the self-supporting phase xylem in other species as well still needs to be verified.

Although lianescent xylem formation was initially related to stem hydraulic demands with crown development (Schenck, 1893), this relationship was found weak or nonexistent later (Obaton, 1960, Ewers *et al.*, 1991). The mechanical role initially performed by the self-supporting xylem and the subsequent relaxation of this function represented by external support attachment was highlighted by Ewers *et al.* (1991) and further explored later (Rowe & Speck, 1996, Gallenmuller *et al.*, 2001; Ménard *et al.*, 2009). The sequence of events observed in shoots of *B. magnifica*, firstly attaching itself to supports and only later increasing in growth, and the formation of lianescent xylem

mostly in supported cultivated branches, corroborates the dependency on external stimuli for the formation of lianescent xylem.

The first evidences of the beginning of lianescent xylem formation was the production of vessels alternating with the protoxylem poles and radial rows of vessels, as well as the production of large vessels. The presence of large and small vessels produced a bimodal distribution of vessel diameter classes. Such a bimodal distribution of vessel diameter classes is not usual in lianas (Ewers *et al.*, 1990, Carlquist, 1991) and should not be assumed due to the term vessel dimorphism (Carlquist, 1981), a common feature in lianescent vascular syndrome. The production of large vessels was also responsible for the increase found in vessel mean diameter, hydraulic diameter, vessel area proportion and the huge increase in specific conductivity (K_s), of more than 22 folds. Although K_s estimation through Hagen-Poiseuille equation overestimates conductivity by disregarding finite vessel size, flow through pits membrane, and internal vessel wall irregularities (Tyree & Ewers, 1991; Lovisolo & Schubert, 1998; Tyree & Zimmermann, 2002), proportionality between calculated K_s and experimentally measured conductivity enables its use for intra and interspecific comparisons (Martre *et al.*, 2000; 2001, Tyree & Zimmermann, 2002; Steppe & Lemeur, 2007).

Despite not being considered in the Hagen-Poiseuille equation, the increase in pit diameter might also impact hydraulic conductivity. This is because pits conductivity resistance account for about 80% of the total resistance (Choat et al., 2006), and larger pits could increase intervessel conductivity. The larger number of vessels per grouping in the lianescent xylem, evidenced by the higher value of the vessel grouping index, also enables alternative paths to water flow, which increases hydraulic safety by maintaining flow in cases of embolism (Carlquist, 1985; Ewers *et al.*, 2007).

The scanty parenchyma associated with the vessels is characteristic of the Bignonieae tribe and its presence is correlated to the presence of septate fibers in the family (Pace & Angyalossy, 2013). These fibers are long-lived cells and can accumulate starch and other compounds (Carlquist, 2001), thus functioning also as a reserve tissue. Both the decrease in fiber and the increase in axial parenchyma proportions are related to the increase in vessel area proportion in lianescent xylem. The heterogeneous ray cell composition is characteristic of the tribe, composed mostly of lianas, and also seems to be common to lianas in general (Pace & Angyalossy, 2013, Angyalossy *et al.*, 2015). The increase in the proportion of procumbent cells in the rays is difficult to interpret functionally but can be related as the transition from a juvenile to a mature phase (Carlquist, 1962).

Self-Supporting Phase Transcriptome is Characterized by the Overexpression of Cell Division and Cell Wall Related Transcripts

The differentiation of self-supporting and lianescent xylem is explained by the differential expression pattern of cambial zone. Our results have clearly shown that self-supporting xylem, composed mostly of fibers and with small diameter vessels, produces higher number of cells per area and has an enhanced growth in thickness, indicating a more active cell division when compared to the lianescent counterpart. In accordance, the self-supporting xylem cambium showed upregulated expression of cyclin-homologous genes responsible for cell cycle progression (TRINITY_DN860_c0_g2_i2, Espinosa-Ruiz *et al.*, 2004) (transcript identifiers hereafter mentioned are listed in Supporting Information Table S4), mitotic specific kinesin homologs (TRINITY_DN13653_c1_g1_i1, TRINITY_DN12012_c0_g1_i1, TRINITY_DN11506_c0_g1_i1, TRINITY_DN13654_c0_g1_i2, Vanstraelen *et al.*, 2006) and chromatin segregation

related proteins (TRINITY_DN1459_c0_g2_i1, De Storme & Geelen 2011, TRINITY_DN5155_c0_g1_i1, Sanchez-Moran *et al.*, 2008; TRINITY_DN19359_c0_g1_i1, Zamariola *et al.*, 2014; TRINITY_DN5075_c0_g1_i1, Antosch *et al.*, 2015) (Fig. 11). It is expected that higher number of cells correlates with more abundant cell wall biosynthesis. In this sense, three master MYB transcription factors (TFs) involved in the regulation of SCW biosynthesis (TRINITY_DN20428_c0_g1_i1, TRINITY_DN7293_c0_g2_i4, TRINITY_DN35518_c0_g1_i1, Yang *et al.*, 2007; 2017; Cassan-Wang *et al.*, 2013; Nakano *et al.*, 2015) were found to be overexpressed in self-supporting xylem forming cambium. Moreover, higher expression levels of genes involved in cell wall biosynthesis, such as cellulose synthase A (CESA7, TRINITY_DN8977_c0_g2_i4, Taylor *et al.*, 2003), and lignification, peroxidase 11 (TRINITY_DN30734_c0_g1_i1, Boerjan *et al.*, 2003) was identified, highlighting the pronounced cell wall deposition. The higher expression of CESA7 is accompanied by the higher expression of four fasciclin-like arabinogalactan proteins (TRINITY_DN7969_c0_g1_i2, TRINITY_DN52901_c0_g1_i1, TRINITY_DN49576_c0_g1_i1, TRINITY_DN10033_c0_g1_i1) that have been proposed to contribute to stem strength and stiffness in *Eucalyptus* and *A. thaliana* by increasing cellulose synthesis and deposition, as well as by composing the extracellular matrix as an adhesion molecule (Macmillan *et al.*, 2010).

Interestingly, two SPIRAL1-like transcripts (TRINITY_DN1885_c0_g1_i2 and TRINITY_DN7226_c0_g1_i1) were found to be overexpressed in self-supporting xylem forming tissue. In *A. thaliana*, SPIRAL1 (SPR1) has been reported to be required for the anisotropic cell growth by determining the correct arrangement of cortical microtubules in rapidly expanding cells, transversally to the major axis (Nakajima *et al.*, 2004; Smyth,

2016). SPR1 overexpression may increase cell elongation, in accordance with the longer fibers found in self-supporting xylem, while SPR1 loss of function mutants show helical growth of epidermal cells and organs as a whole (Nakajima *et al*., 2004), as has long been known in twinning vines stems (Darwin, 1875; Isnard & Silk, 2009). Other cell growth related proteins overexpressed in our study were four homologs to expansins (TRINITY_DN5405_c0_g1_i2, TRINITY_DN57873_c0_g1_i1, TRINITY_DN3738_c0_g1_i2, and TRINITY_DN8582_c0_g1_i3), three of which were overexpressed in the self-supporting phase, and one in the lianescent phase. Expansins form a large gene family, whose members are organ, tissue, or even cell-specific (Gray-Mitsumune *et al*., 2004; Sundell *et al*., 2017). For example, the *Populus* EXPA1 showed to have distinct effects on vessels and fibers, stimulating diameter growth in the last but not in the former, while marginally increases length in vessels, but not in fibers (Gray-Mitsumune *et al.*, 2008). In this way, the differential expression of distinct *B. magnifica* expansin homologs in the two xylem forming cambia analyzed may reflect the anatomical unique cellular characteristics associated with these tissues functional specificity.

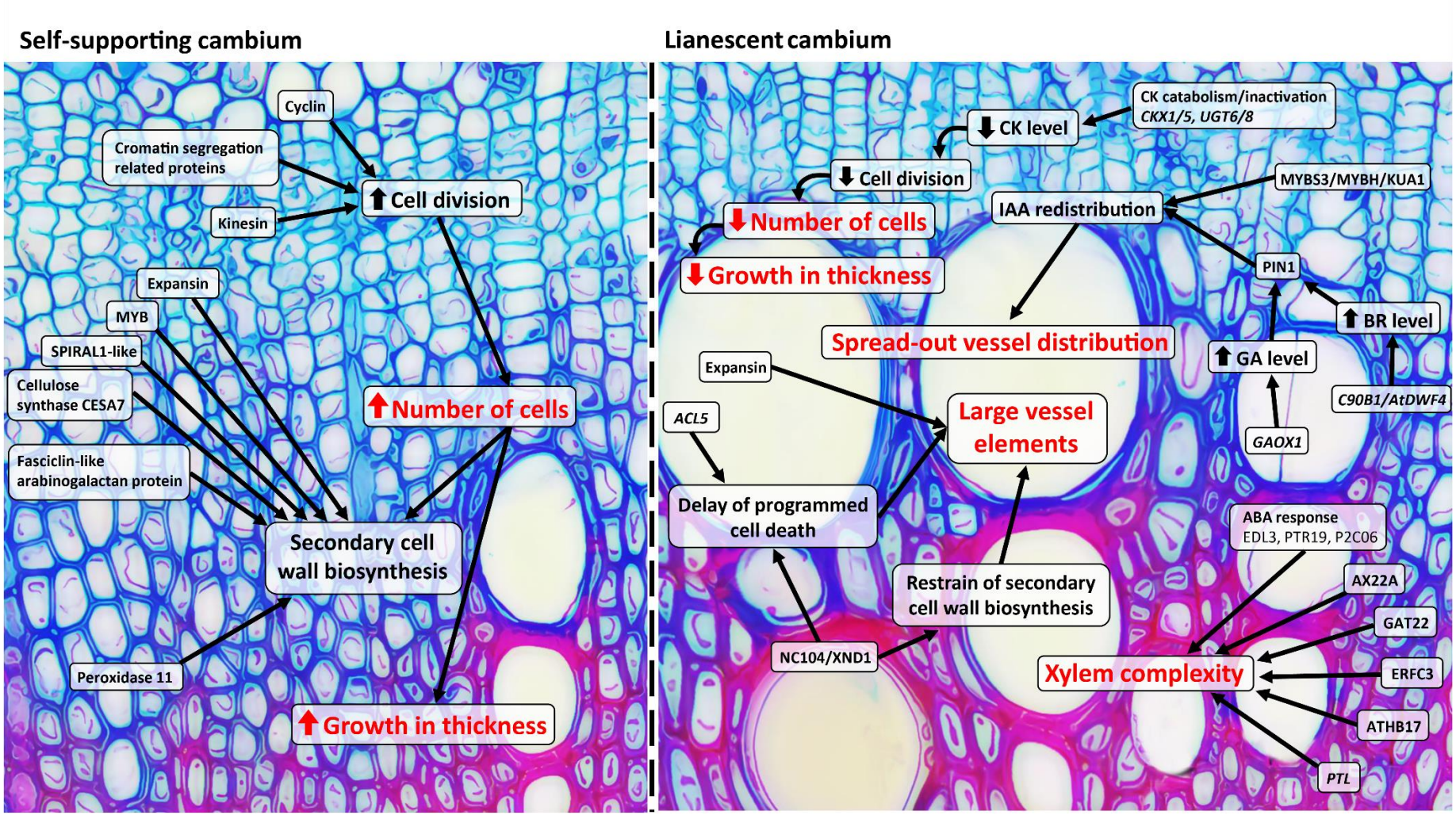
Self-supporting cambium
Cyclin
Cromatin segregation related proteins
Kinesin
Cell division
Expansin
MYB
SPIRAL1-like
Cellulose synthase CESA7
Fasciclin-like arabinogalactan protein
Peroxidase 11
Number of cells
Secondary cell wall biosynthesis
Growth in thickness
Lianescent cambium
CK catabolism/inactivation
CKX1/5, UGT6/8
CK level
Cell division
Number of cells
Growth in thickness
MYBS3/MYBH/KUA1
IAA redistribution
PIN1
BR level
Spread-out vessel distribution
GA level
C90B1/AtDWF4
Expansin
ACL5
Large vessel elements
GAOX1
Delay of programmed cell death
ABA response
EDL3, PTR19, P2C06
Restrain of secondary cell wall biosynthesis
AX22A
GAT22
NC104/XND1
Xylem complexity
ERFC3
ATHB17
PTL

Lianescent Phase Transcriptome is Characterized by the Overexpression of Response to Stimulus, Hormone Responsive and Defense/Cell Death Related Transcripts

Lianescent phase has an evident more complex xylem than the homogeneous self-supporting phase. It shows vessel dimorphism, with wider vessels that constitute a larger proportion of the xylem, solitary or associated with small tracheary elements, and are not restricted to the radial arrangement lined to the protoxylem poles. This is the reflex of an also more complex transcriptional pattern as shown by the higher number of transcripts associated to TFs and hormone response in our hand curated annotation among lianescent phase overexpressed DEGs (Fig. 11).

NAC and MYB TFs act as first- and second-level master switches regulating SCW deposition (J. Zhang *et al.*, 2014; Ye & Zhong, 2015). TRINITY_DN10071_c0_g1_i1, which was overexpressed in lianescent xylem, is homolog to the *A. thaliana* NAC DOMAIN-CONTAINING PROTEIN 104/ XYLEM NAC DOMAIN 1 (NC104/XND1 NAC**)** domain-containing protein, which was found to interact with first-level master regulator NAC SECONDARY WALL THICKENING PROMOTING FACTOR1 (NST1), impairing both cell wall production and programmed cell death (PCD) (Zhao *et al.*, 2008; Q. Zhang *et al.*, 2019). SCW production and PCD are transcriptionally

Fig. 11 (*previous* page) Transcriptional regulatory network model of self-supporting and lianescent xylem formation in the stems of the liana *B. magnifica*. Self-supporting xylem has a higher growth in thickness rate and is composed mainly by fibers and small vessel arranged in radial rows in front of protoxylem poles. Its formation is associated to a higher expression of cell division and secondary cell wall biosynthesis related transcripts. Lianescent xylem has a slower growth in thickness and is composed by a smaller fraction of fibers and a higher proportion of vessels. This change is due to the production of large vessels, which are produced throughout cambium circumference. The formation of lianescent xylem is linked to a much more complex transcription network, involving transcription factors, hormone responsive genes, delayed programmed cell death and redistribution of auxin mediated by PIN proteins.

coregulated as components of a broad xylem maturation program, what denotes the importance of accurate PCD timing for the correct cellular differentiation and function (Bollhoner *et al.*, 2012). Interestingly, another gene responsible for preventing premature PCD, *ACAULIS5* (*ACL5*) (Muñiz *et al.*, 2008), was overexpressed in the lianescent xylem, although with a log2 fold change of 1.1. The increase in cell expansion time span, prior to PCD, was found to be linearly correlated with tracheid lumen area in *Picea abies* trees (Anfodillo *et al.*, 2013), and explains, at least in part, the wider size of the vessels in lianescent xylem. Similarly, the overrepresentation of genes associated with defense/cell death is probably related with the more pronounced vessel elements differentiation observed in lianescent xylem, as fibers of both self-supporting and lianescent phases are septate, staying alive at maturity (Carlquist, 2001). A homolog of the *A. thaliana* MYBS3/MYBH/KUODA1 protein was also overexpressed in lianescent xylem cambium. This TF has shown to trigger auxin (IAA) accumulation inducing cellular elongation (Kwon *et al.*, 2013, Lu *et al.*, 2014), which might contribute to the differentiation of larger vessels.

Other transcripts, homologs to TF encoding mRNAs essential for vascular development were found overexpressed in lianescent cambium. The upregulation of a *PETAL LOSS* (*PTL*) homolog (TRINITY_DN52789_c0_g1_i1) is in agreement to the reduced number of cell found in the lianescent xylem, since PTL was recently characterized as a repressor of cell proliferation during root secondary growth in *A. thaliana* (J. Zhang *et al.*, 2019). Interestingly, a homolog of the *A. thaliana* homeobox-leucine zipper protein ATHB17 was identified as a DEG in lianescent xylem forming meristem (TRINITY_DN11122_c0_g1_i1). This gene belongs to an important TF family acting on vascular differentiation (Baima *et al.*, 2001; Ohashi-Ito *et al.*, 2003).

Transcripts belonging to hormone response category was profoundly upregulated in the lianescent cambium compared to self-supporting counterpart. These genes encompass functions associated with biosynthesis, catabolism/deactivation, transport and signaling pathway for IAA, cytokinins (CK), gibberellins (GA), brassinosteroids (BR), and abscisic acid (ABA). Transcripts homologs to AUXIN-INDUCED PROTEIN 22A (AX22A) (TRINITY_DN53387_c0_g1_i1), GATA TRANSCRIPTION FACTOR 22 (GAT22) (TRINITY_DN16098_c0_g1_i1) and ETHYLENE-RESPONSIVE TRANSCRIPTION FACTOR 1B (ERFC3) (TRINITY_DN35952_c0_g1_i1) TFs that are involved in the response to the cambial activity regulating hormones AIA, CK and ethylene, respectively, were identified between the lianescent cambium DEGs, showing the greater complexity of cell differentiation regulation in this xylem.

CK was the hormone with the highest number of related annotated transcripts overexpressed. Four out of the five mRNAs were related to CK catabolism/deactivation (TRINITY_DN20233_c0_g1_i1, TRINITY_DN9178_c0_g1_i1, TRINITY_DN17065_c0_g1_i1, TRINITY_DN49211_c0_g1_i1) and are homologs to *A. thaliana CYTOKININ DEHYDROGENASE 1* and *5* (*CKX1/5*), and *UDP-GLYCOSYLTRANSFERASE 85A3* and *85A1* (*UGT6/8*). The product of these genes might lead to lower levels of CKs resulting in reduced cambial cell divisions in the lianescent xylem meristem phase. CKs, in association with IAA, have been long known to act in cambial activity (Torrey & Loomis, 1967). The *A. thaliana* quadruple mutant *atip1/3/5/7*, deficient for CK biosynthesis, failed to form cambium and showed reduced secondary growth (Matsumoto-Kitano *et al.*, 2008), while a transgenic *Populus* overexpressing a single CK catabolic gene showed reduced concentration of bioactive CKs and scanty thickness growth (Nieminen *et al.*, 2008). Intriguingly, one transcript (TRINITY_DN17601_c0_g2_i1) annotated as the CK biosynthetic gene, *ADENYLATE*

ISOPENTENYLTRANSFERASE 3, was also overexpressed in this phase. Similarly, we found that *GA20 OXIDASE 1* (*GAOX1*), a late GA biosynthesis gene (Huang *et al.*, 1998), homolog (TRINITY_DN11261_c0_g1_i1) was overexpressed in lianescent xylem forming tissues, in the same way as two other GA responsive transcripts (TRINITY_DN3693_c0_g1_i1, TRINITY_DN12113_c0_g1_i1). GA enhances cambial activity and xylem cell differentiation by promoting class-I *KNOTTED1-LIKE HOMEOBOX* gene (KNOX) *KNAT1* (for *KNOTTED-LIKE FROM ARABIDOPSIS THALIANA*) action through the degradation of the negative regulator DELLA (Israelsson *et al.*, 2005; Mauriat & Moritz, 2009; Felipo-Benavent *et al.*, 2018). Nevertheless, fibers were shorter in lianescent xylem, an opposite character than that sowed by GAOX1 overexpressing *Populus* trees (Eriksson *et al.*, 2000).

Auxin is the major regulatory shoot signal in the differentiation of vascular system (Snow, 1935; Aloni & Jacobs, 1977; Ko *et al.*, 2004; Bjorklund *et al*, 2007; Ye & Zhong, 2015; Smetana *et al.*, 2019). It is produced mainly in leaf primordia (Aloni *et al*., 2003) where a positive feedback loop, determined by PIN-FORMED 1 (PIN1)-mediated polar transport, channels auxin flow, leading to the differentiation of leaf venation pattern (Sachs, 1981; Vieten *et al.*, 2005; Scarpella *et al.*, 2006). In the same way, regenerating wounded tissues express PIN1 in cells that will later differentiate in regenerative vessels bypassing the wound (Mazur *et al.*, 2016). In the stem, PIN1 is initially expressed only in the vascular bundles, and just later in cambium and cambium differentiating interfascicular parenchyma, where auxin concentration peaks (Uggla *et al.*, 1996; Tuominen *et al.*, 1997; Mazur *et al.*, 2014). Although, the role of PIN1 auxin carrier in *de novo* bundle differentiation has been extensively reported, its role in secondary vessel formation has never been shown. Here, we found a PIN1 homolog, TRINITY_DN10775_c0_g1_i1, overexpressed in lianescent xylem forming cambium

that might reflect the higher number of PIN1 expressing vessel elements-differentiating xylem mother cells leading to the spread-out vessel distribution observed. Although the overall vessel concentration did not vary, the maximum number of vessels being formed at any given time in the self-supporting xylem was equal to the number of the few radial rows of vessels opposite to protoxylem poles, while in the lianescent xylem vessels were produced many at a time by a much broader range of cambial initials. This same argument explains the upregulation of transcripts annotated as defense/cell death related in our hand-curated annotation, as vessel elements, different from the septate-fibers, are the only xylem cell type subjected to programed cell death (PCD). We also do not overlook the possibility that some of the defense-related genes are eventually involved with the presence of endophytic parasites.

Lianescent cambium still showed a higher expression of the brassinosteroid (BR) biosynthetic gene homolog *CYTOCHROME P450 90B1/DWARF4* (*C90B1/AtDWF4*; TRINITY_DN4579_c0_g1_i1, Sahni *et al.*, 2016; Fujiyama *et al.*, 2019), and four ABA responsive transcripts; three of which are involved in signaling pathway: EID1-LIKE F-BOX PROTEIN 3, (EDL3, PTR19, P2C06 (TRINITY_DN45297_c0_g1_i1, TRINITY_DN10749_c0_g1_i1, TRINITY_DN10194_c0_g1_i5) (Koops *et al.*, 2011; Kanno *et al.*, 2012; Saez *et al.*, 2004; Yoshida *et al.*, 2006). BR are plant steroid hormones that have been also reported to be involved in xylem differentiation and phloem repression (Yamamoto *et al.*, 1997; 2001; Caño-Delgado *et al.*, 2004), besides to stimulate ethylene production, and modify endogenous auxin distribution by enhancing polar accumulation of PIN2 in a RHO-OF-PLANT GTPASE (ROP2) dependent way (Li *et al.*, 2005). Although ABA activity in xylem differentiation remains poorly understood, it might contribute to control xylem cell expansion by regulating the expression of cell wall modifying genes (Little & Wareing, 1981; Luisi *et al.*, 2014).

The arguments exposed above demonstrate an intricate network that controls cell division and differentiation that finally results in a much more complex antomy in lianescent xylem.

Conclusions

In the present study, we verified profound impacts of support on the liana *B. magnifica* shoot development, increasing growth in length, decreasing growth in thickness and promoting the formation of the lianescent xylem. The detailed xylem anatomical characterization showed that the onset of lianescent phase is characterized by much larger vessels, whose production is not anymore restricted to the front of protoxylem poles, that drastically increase specific conductivity. The comprehensive integration of anatomical and differential expression analysis data allows us to propose a model to characterize the molecular control of the lianescent vascular syndrome establishment (Fig 11). Our model shows that the more complex lianescent xylem reflects an also more intricate transcriptional regulation network, involving a more diverse repertory of transcription factors and hormone responsive genes.

References

Agusti, J., Herold, S., Schwarz, M., Sanchez, P., Ljung, K., Dun, E. A., ... & Greb, T. 2011. Strigolactone signaling is required for auxin-dependent stimulation of secondary growth in plants. *Proceedings of the National Academy of Sciences*, *108*(50), 20242-20247.

Aloni, R., & Jacobs, W. P. 1977. Polarity of tracheary regeneration in young internodes of Coleus (Labiatae). *American Journal of Botany*, *64*(4), 395-403.

Aloni, R., Schwalm, K., Langhans, M., & Ullrich, C. I. 2003. Gradual shifts in sites of free-auxin production during leaf-primordium development and their role in vascular differentiation and leaf morphogenesis in Arabidopsis. *Planta*, *216*(5), 841-853.

Anfodillo, T., Petit, G., & Crivellaro, A. 2013. Axial conduit widening in woody species: a still neglected anatomical pattern. *Iawa Journal*, *34*(4), 352-364.

Angyalossy, V., Angeles, G., Pace, M. R., Lima, A. C., Dias-Leme, C. L., Lohmann, L. G., & Madero-Vega, C. 2012. An overview of the anatomy, development and evolution of the vascular system of lianas. *Plant Ecology & Diversity*, *5*, 167-182.

Angyalossy, V., Pace, M. R., & Lima, A. C. 2015. Liana anatomy: a broad perspective on structural evolution of the vascular system. In Schnitzer, S. A., Bongers, F., Burnham, R. J. & Putz, F. E. (eds.). Ecology of Lianas. John Wiley & Sons Ltd. Chichester.

Antosch, M., Schubert, V., Holzinger, P., Houben, A., & Grasser, K. D. 2015. Mitotic lifecycle of chromosomal 3x HMG-box proteins and the role of their N-terminal domain in the association with r DNA loci and proteolysis. *New Phytologist*, *208*(4), 1067-1077.

Baas, P., Ewers, F. W., Davis, S. D., & Wheeler, E. A. 2004. Evolution of xylem physiology. In Hemsley, A. R., Poole, I. (eds.). The Evolution of Plant Physiology. Elsevier Academic Press, London.

Baas, P., Schmid, R., & van Heuven, B. J. 1986. Wood anatomy of Pinus longaeva (bristlecone pine) and the sustained length-on-age increase of its tracheids. *IAWA Journal*, *7*(3), 221-228.

Bailey, I. W., & Tupper, W. W. 1918. Size variation in tracheary cells: I. A comparison between the secondary xylems of vascular cryptogams, gymnosperms and angiosperms. *Proceedings of the American Academy of Arts and Sciences, 54* (2), 149-204.

Baima, S., Possenti, M., Matteucci, A., Wisman, E., Altamura, M. M., Ruberti, I., & Morelli, G. 2001. The Arabidopsis ATHB-8 HD-zip protein acts as a differentiation-promoting transcription factor of the vascular meristems. *Plant physiology*, *126*(2), 643-655.

Barbosa, A. C. F., Pace, M. R., Witovsk, L., & Angyalossy, V. 2010. A new method to obtain good anatomical slides of heterogeneous plant parts. *IAWA Journal, 31*, 373-383.

Becker, P., Gribben, R. J., & Lim, C. M. 2000. Tapered conduits can buffer hydraulic conductance from path-length effects. *Tree Physiology*, *20*(14), 965-967.

Beeckman, H. 2016. Wood anatomy and trait-based ecology. *IAWA journal*, *37*(2), 127-151.

Bergander, A., & Salmén, L. 2002. Cell wall properties and their effects on the mechanical properties of fibers. *Journal of materials science*, *37*(1), 151-156.

Berlyn, G. P., & Miksche J. P. 1976. Botanical microtechnique and cytochemistry. Iowa State University Press, Ames.

Beyer, M., Nazareno, A. G., & Lohmann, L. G. 2019. Development of nuclear microsatellite markers in Stizophyllum (Bignoniaceae) using next-generation sequencing. *Plant Genetic Resources*, 1-4.

Bittencourt, P. R., Pereira, L., Oliveira, R. S. 2016. On xylem hydraulic efficiencies, wood space-use and the safety–efficiency tradeoff: comment on Gleason *et al.* (2016) 'Weak tradeoff between xylem safety and xylem-specific hydraulic efficiency across the world's woody plant species'. *New Phytologist* 211:1152–1155.

Björklund, S., Antti, H., Uddestrand, I., Moritz, T., & Sundberg, B. 2007. Cross-talk between gibberellin and auxin in development of Populus wood: gibberellin stimulates polar auxin transport and has a common transcriptome with auxin. *The Plant Journal*, *52*(3), 499-511.

BLAST® Command Line Applications User Manual [Internet]. Bethesda (MD): National Center for Biotechnology Information (US); 2008-. Available from: https://www.ncbi.nlm.nih.gov/books/NBK279690/

Boerjan, W., Ralph, J., & Baucher, M. 2003. Lignin biosynthesis. *Annual review of plant biology*, *54*(1), 519-546.

Bollhöner, B., Prestele, J., & Tuominen, H. 2012. Xylem cell death: emerging understanding of regulation and function. *Journal of Experimental Botany*, *63*(3), 1081-1094.

Bourmaud, A., Morvan, C., Bouali, A., Placet, V., Perre, P., & Baley, C. 2013. Relationships between micro-fibrillar angle, mechanical properties and biochemical composition of flax fibers. *Industrial Crops and Products*, *44*, 343-351.

Bukatsch, F. 1972. Bemerkungem zur Doppelfärbung Astra-blau-Safranin. Mikrokosmos 6:255.

Burnham, R.J. 2009. An overview of the fossil record of climbers: bejucos, sogas, trepadoras, lianas, cipós, and vines. *Revista Brasileira de Paleontologia*, *12*, 149–160.

Caballé, G. U. Y. 1993. Liana structure, function and selection: a comparative study of xylem cylinders of tropical rainforest species in Africa and America. *Botanical Journal of the Linnean Society*, *113*(1), 41-60.

Caballé, G. 1998. Le port autoportant des lianes tropicales: une synthèse des stratégies de croissance. *Canadian Journal of Botany*, *76*, 1703-1716.

Cabanillas, P. A., Pace, M. R., & Angyalossy, V. 2017. Structure and ontogeny of the fissured stems of Callaeum (Malpighiaceae). *IAWA Journal*, *38*(1), 49-66.

Caño-Delgado, A., Yin, Y., Yu, C., Vafeados, D., Mora-García, S., Cheng, J. C., ... & Chory, J. 2004. BRL1 and BRL3 are novel brassinosteroid receptors that function in vascular differentiation in Arabidopsis. *Development*, *131*(21), 5341-5351.

Carlquist, S. 1962. A theory of paedomorphosis in dicotyledonous woods. *Phytomorphology*, *12*(1), 30-45.

Carlquist, S. 1981. Wood anatomy of Nepenthaceae. *Bulletin of the Torrey Botanical Club*, *108*, 324-330.

Carlquist, S. 1985. Observations on functional wood histology of vines and lianas: vessel dimorphism, tracheids, vasicentric tracheids, narrow vessels, and parenchyma. *Aliso 11*, 139-157.

Carlquist, S. 1991. Anatomy of vine and liana stems: a review and synthesis. In Putz, F. E. & Mooney, H.A. (eds.). The Biology of Vines. Cambridge University Press, Cambrige.

Carlquist, S. 2001. Comparative Wood Anatomy. 2nd ed. Springer, Berlin.

Carpentier, S. C., Panis, B., Vertommen, A., Swennen, R., Sergeant, K., Renaut, J., ... & Devreese, B. 2008. Proteome analysis of non-model plants: a challenging but powerful approach. *Mass spectrometry reviews*, *27*(4), 354-377.

Cassan-Wang, H., Goué, N., Saidi, M. N., Legay, S., Sivadon, P., Goffner, D., & Grima-Pettenati, J. 2013. Identification of novel transcription factors regulating secondary cell wall formation in Arabidopsis. *Frontiers in plant science*, *4*, 189.

Choat, B., Brodie, T. W., Cobb, A. R., Zwieniecki, M. A., & Holbrook, N. M. 2006. Direct measurements of intervessel pit membrane hydraulic resistance in two angiosperm tree species. *American journal of botany*, 93(7), 993-1000.

Conesa, A., Götz, S., García-Gómez, J. M., Terol, J., Talón, M., & Robles, M. 2005. Blast2GO: a universal tool for annotation, visualization and analysis in functional genomics research. *Bioinformatics*, *21*(18), 3674-3676.

Cordeiro, J. M., Kaehler, M., Souza, G., & Felix, L. P. 2017. Karyotype analysis in Bignonieae (Bignoniaceae): chromosome numbers and heterochromatin. *Anais da Academia Brasileira de Ciências*, *89*(4), 2697-2706.

Costa, S. L., Brito, I. J. N., Lohmann, L. G., & de Melo, J. I. M. 2019. New records of the tribe Bignonieae (Bignoniaceae) for Paraiba state, northeastern Brazil. *Acta Brasiliensis*, *3*(3), 89-96.

Crawley, M. J. 2007. The R Book. London, John Wiley & Sons Ltd..

Darwin, C. 1875. *The movements and habits of climbing plants*. J. Murray, London, UK.

De Storme, N., & Geelen, D. 2011. The Arabidopsis mutant jason produces unreduced first division restitution male gametes through a parallel/fused spindle mechanism in meiosis II. *Plant physiology*, *155*(3), 1403-1415.

Dos Santos, G. M. A. 1995. Wood anatomy, chloroplast DNA, and flavonoids of the tribe Bignonieae (Bignoniaceae). PhD thesis, University of Reading, Reading, UK.

Duarte, M. O., Mendes-Rodrigues, C., Alves, M. F., Oliveira, P. E., & Sampaio, D. S. 2017. Mixed pollen load and late-acting self-incompatibility flexibility in Adenocalymma

peregrinum (Miers) LG Lohmann (Bignonieae: Bignoniaceae). *Plant Biology*, *19*(2), 140-146.

Eriksson, M. E., Israelsson, M., Olsson, O., & Moritz, T. 2000. Increased gibberellin biosynthesis in transgenic trees promotes growth, biomass production and xylem fiber length. *Nature biotechnology*, *18*(7), 784.

Espinosa-Ruiz, A., Saxena, S., Schmidt, J., Mellerowicz, E., Miskolczi, P., Bakó, L., & Bhalerao, R. P. 2004. Differential stage-specific regulation of cyclin-dependent kinases during cambial dormancy in hybrid aspen. *The Plant Journal*, *38*(4), 603-615.

Evert, R. F. 2006. *Esau's plant anatomy: meristems, cells, and tissues of the plant body: their structure, function, and development*. John Wiley & Sons.

Ewers, F. W., Ewers, J. M., Jacobsen, A. L., & López-Portillo, J. 2007. Vessel redundancy: modeling safety in numbers. *Iawa Journal*, 28(4), 373-388.

Ewers, F. W., & Fisher, J. B. 1989. Variation in vessel length and diameter in stems of six tropical and subtropical lianas. *American Journal of Botany*, *76*(10), 1452-1459.

Ewers, F. W., Fisher, J. B., & Chiu, S. T. 1990. A survey of vessel dimensions in stems of tropical lianas and other growth forms. *Oecologia*, *84*(4), 544-552.

Ewers, F. W., Fisher, J. B., Fichtner, K. 1991. Water flux and xylem structure in vines. In Putz, F. E. & Mooney, H. A. (eds.). The Biology of Vines. Cambridge University Press, Cambridge.

Felipo-Benavent, A., Úrbez, C., Blanco-Touriñán, N., Serrano-Mislata, A., Baumberger, N., Achard, P., ... & Alabadí, D. 2018. Regulation of xylem fiber differentiation by gibberellins through DELLA-KNAT1 interaction. *Development*, *145*(23).

Fonseca, L. H. M., Cabral, S. M., Agra, M. D. F., & Lohmann, L. G. 2017. Taxonomic revision of Dolichandra (Bignonieae, Bignoniaceae). *Phytotaxa*, *301*(1), 1-70.

Fujiyama, K., Hino, T., Kanadani, M., Watanabe, B., Lee, H. J., Mizutani, M., & Nagano, S. 2019. Structural insights into a key step of brassinosteroid biosynthesis and its inhibition. *Nature plants*, *5*(6), 589.

Gallenmüller, F., Müller, U., Rowe, N., & Speck, T. 2001. The Growth Form of Croton pullei (Euphorbiaceae)-Functional Morphology and Biomechanics of a Neotropical Liana. *Plant Biology*, *3*(1), 50-61.

Gartner, B. L. 1991**a**. Relative growth rates of vines and shrubs of western poison oak, Toxicodendron diversilobum (Anacardiaceae). *American Journal of Botany, 78(10)*, 1345-1353.

Gartner, B. L. 1995. Patterns of xylem variation within a tree and their hydraulic and mechanical consequences. In *Plant stems* (pp. 125-149). Academic Press.

Gentry, A. H. 1973. Generic delimitations of central American Bignoniaceae. *Brittonia*, *25*(3), 226-242.

Gentry, A. H. 1980. Bignoniaceae: Part I (Crescentieae and Tourrettieae). *Flora Neotropica*, *25*(1), 1-130.

Gentry, A. H. 1986. Species richness and floristic composition of Chocó region plant communities. *Caldasia*, 71-91.

Gentry, A. H. 1991. The distribution and evolution of climbing plants. In Putz, F. E. & Mooney, H. A. (eds.). The Biology of Vines. Cambridge University Press, Cambridge.

Gerolamo, C. S., & Angyalossy, V. 2017. Wood anatomy and conductivity in lianas, shrubs and trees of Bignoniaceae. *IAWA Journal*, *38*(3), 412-432.

Gray-Mitsumune, M., Blomquist, K., McQueen-Mason, S., Teeri, T. T., Sundberg, B., & Mellerowicz, E. J. 2008. Ectopic expression of a wood-abundant expansin PttEXPA1 promotes cell expansion in primary and secondary tissues in aspen. *Plant biotechnology journal*, *6*(1), 62-72.

Gray-Mitsumune, M., Mellerowicz, E. J., Abe, H., Schrader, J., Winzéll, A., Sterky, F., ... & Sundberg, B. 2004. Expansins abundant in secondary xylem belong to subgroup A of the α-expansin gene family. *Plant Physiology*, *135*(3), 1552-1564.

Groover, A. T. 2005. What genes make a tree a tree?. *Trends in plant science*, *10*(5), 210-214.

Haas, B. J., Papanicolaou, A., Yassour, M., Grabherr, M., Blood, P. D., Bowden, J., ... & MacManes, M. D. 2013. De novo transcript sequence reconstruction from RNA-seq using the Trinity platform for reference generation and analysis. *Nature protocols*, *8*(8), 1494.

Hacke, U. G., Spicer, R., Schreiber, S. G., & Plavcová, L. 2017. An ecophysiological and developmental perspective on variation in vessel diameter. *Plant, cell & environment*, *40*(6), 831-845.

Hirakawa, Y., Kondo, Y., & Fukuda, H. 2010. TDIF peptide signaling regulates vascular stem cell proliferation via the WOX4 homeobox gene in Arabidopsis. *The Plant Cell*, *22*(8), 2618-2629.

Hu, R., Qi, G., Kong, Y., Kong, D., Gao, Q., & Zhou, G. 2010. Comprehensive analysis of NAC domain transcription factor gene family in Populus trichocarpa. *BMC plant biology*, *10(1)*, 145.

Huang, S., Raman, A. S., Ream, J. E., Fujiwara, H., Cerny, R. E., & Brown, S. M. 1998. Overexpression of 20-oxidase confers a gibberellin-overproduction phenotype in Arabidopsis. *Plant physiology*, *118*(3), 773-781.

Huber, W., Carey, V. J., Gentleman, R., Anders, S., Carlson, M., Carvalho, B. S., ... & Gottardo, R. 2015. Orchestrating high-throughput genomic analysis with Bioconductor. *Nature methods*, *12*(2), 115.

IAWA Committee 1989. IAWA list of microscopic features for hardwood identification.

Isnard, S., & Silk, W. K. 2009. Moving with climbing plants from Charles Darwin's time into the 21st century. *American Journal of Botany*, *96*(7), 1205-1221.

Israelsson, M., Sundberg, B., & Moritz, T. 2005. Tissue-specific localization of gibberellins and expression of gibberellin-biosynthetic and signaling genes in wood-forming tissues in aspen. *The Plant Journal*, *44*(3), 494-504.

Johansen, D.A. 1940. Plant microtechinique. McGraw - Hill Book Co. Inc., New York.

Kaehler, M., Michelangeli, F. A., & Lohmann, L. G. 2019. Fine tuning the circumscription of Fridericia (Bignonieae, Bignoniaceae). *Taxon*, *68*(4), 751-770.

Kanno, Y., Hanada, A., Chiba, Y., Ichikawa, T., Nakazawa, M., Matsui, M., ... & Seo, M. 2012. Identification of an abscisic acid transporter by functional screening using the receptor complex as a sensor. *Proceedings of the National Academy of Sciences*, *109*(24), 9653-9658.

Kans, J. 2018. Entrez direct: E-utilities on the UNIX command line. In, Entrez Programming Utilities Help [Internet]. *National Center for Biotechnology Information (US). https://www. ncbi. nlm. nih. gov/books/NBK179288/. Published*.

Kim, D., Langmead, B., & Salzberg, S. L. 2015. HISAT: a fast spliced aligner with low memory requirements. *Nature methods*, *12*(4), 357.

Ko, J. H., Han, K. H., Park, S., & Yang, J. 2004. Plant body weight-induced secondary growth in Arabidopsis and its transcription phenotype revealed by whole-transcriptome profiling. *Plant Physiology*, *135*(2), 1069-1083.

Ko, J. H., Kim, W. C., & Han, K. H. 2009. Ectopic expression of MYB46 identifies transcriptional regulatory genes involved in secondary wall biosynthesis in Arabidopsis. *The Plant Journal*, *60(4)*, 649-665.

Koops, P., Pelser, S., Ignatz, M., Klose, C., Marrocco-Selden, K., & Kretsch, T. 2011. EDL3 is an F-box protein involved in the regulation of abscisic acid signalling in Arabidopsis thaliana. *Journal of experimental botany*, *62*(15), 5547-5560.

Kubo, M., Udagawa, M., Nishikubo, N., Horiguchi, G., Yamaguchi, M., Ito, J., ... & Demura, T. 2005. Transcription switches for protoxylem and metaxylem vessel formation. Genes & development, 19(16), 1855-1860.

Kwon, Y., Kim, J. H., Nguyen, H. N., Jikumaru, Y., Kamiya, Y., Hong, S. W., & Lee, H. 2013. A novel Arabidopsis MYB-like transcription factor, MYBH, regulates hypocotyl elongation by enhancing auxin accumulation. *Journal of experimental botany*, *64*(12), 3911-3922.

Li, L., Xu, J., Xu, Z. H., & Xue, H. W. 2005). Brassinosteroids stimulate plant tropisms through modulation of polar auxin transport in Brassica and Arabidopsis. The Plant Cell, 17(10), 2738-2753.

Li, X., Yang, Y., Yao, J., Chen, G., Li, X., Zhang, Q., & Wu, C. 2009. FLEXIBLE CULM 1 encoding a cinnamyl-alcohol dehydrogenase controls culm mechanical strength in rice. *Plant molecular biology*, *69*(6), 685-697.

Little, C. H. A., & Wareing, P. F. 1981. Control of cambial activity and dormancy in Picea sitchensis by indol-3-ylacetic and abscisic acids. *Canadian Journal of Botany*, *59*(8), 1480-1493.

Lohmann, L. G. 2006. Untangling the phylogeny of neotropical lianas (Bignonieae, Bignoniaceae). *American Journal of Botany*, 93(2), 304-318.

Lohmann, L. G., Bell, C. D., Calió, M. F., & Winkworth, R. C. 2012. Pattern and timing of biogeographical history in the Neotropical tribe Bignonieae (Bignoniaceae). *Botanical Journal of the Linnean Society*, *171*(1), 154-170.

Lohmann, L. G., & Taylor, C. M. 2014. A new generic classification of tribe Bignonieae (Bignoniaceae) 1. *Annals of the Missouri Botanical Garden*, *99*(3), 348-489.

Lovisolo, C., & Schubert, A. 1998. Effects of water stress on vessel size and xylem hydraulic conductivity in Vitis vinifera L. *Journal of experimental botany*, *49*(321), 693-700.

Lu, D., Wang, T., Persson, S., Mueller-Roeber, B., & Schippers, J. H. 2014. Transcriptional control of ROS homeostasis by KUODA1 regulates cell expansion during leaf development. Nature communications, 5, 3767.

Luisi, A., Giovannelli, A., Traversi, M. L., Anichini, M., & Sorce, C. 2014. Hormonal responses to water deficit in cambial tissues of Populus alba L. *Journal of plant growth regulation*, *33*(3), 489-498.

MacMillan, C. P., Mansfield, S. D., Stachurski, Z. H., Evans, R., & Southerton, S. G. 2010. Fasciclin-like arabinogalactan proteins: specialization for stem biomechanics and cell wall architecture in Arabidopsis and Eucalyptus. *The Plant Journal*, *62*(4), 689-703.

Martre, P., Cochard, H., & Durand, J. L. 2001. Hydraulic architecture and water flow in growing grass tillers (Festuca arundinacea Schreb.). *Plant, Cell & Environment*, *24*(1), 65-76.

Martre, P., Durand, J. L., & Cochard, H. 2000. Changes in axial hydraulic conductivity along elongating leaf blades in relation to xylem maturation in tall fescue. *The New Phytologist*, *146*(2), 235-247.

Matsumoto-Kitano, M., Kusumoto, T., Tarkowski, P., Kinoshita-Tsujimura, K., Václavíková, K., Miyawaki, K., & Kakimoto, T. 2008. Cytokinins are central regulators of cambial activity. *Proceedings of the National Academy of Sciences*, *105*(50), 20027-20031.

Mauriat, M., & Moritz, T. 2009. Analyses of GA20ox-and GID1-over-expressing aspen suggest that gibberellins play two distinct roles in wood formation. *The Plant Journal*, *58*(6), 989-1003.

Mazur, E., Benková, E., & Friml, J. 2016. Vascular cambium regeneration and vessel formation in wounded inflorescence stems of Arabidopsis. *Scientific reports*, *6*, 33754.

Mazur, E., Kurczyńska, E. U., & Friml, J. 2014. Cellular events during interfascicular cambium ontogenesis in inflorescence stems of Arabidopsis. *Protoplasma*, *251*(5), 1125-1139.

McCarthy, R. L., Zhong, R., & Ye, Z. H. 2009. MYB83 is a direct target of SND1 and acts redundantly with MYB46 in the regulation of secondary cell wall biosynthesis in Arabidopsis. *Plant and Cell Physiology*, *50(11)*, 1950-1964.

Ménard, L., McKey, D., & Rowe, N. 2009. Developmental plasticity and biomechanics of treelets and lianas in Manihot aff. quinquepartita (Euphorbiaceae): a branch-angle climber of French Guiana. *Annals of Botany*, *103(8)*, 1249-1259.

Meyer, L., Diniz-Filho, J. A. F., Lohmann, L. G., Hortal, J., Barreto, E., Rangel, T., & Kissling, W. D. 2020. Canopy height explains species richness in the largest clade of Neotropical lianas. *Global Ecology and Biogeography*, *29*(1), 26-37.

Muñiz, L., Minguet, E. G., Singh, S. K., Pesquet, E., Vera-Sirera, F., Moreau-Courtois, C. L., ... & Tuominen, H. 2008. ACAULIS5 controls Arabidopsis xylem specification through the prevention of premature cell death. Development, 135(15), 2573-2582.

Nakajima, K., Furutani, I., Tachimoto, H., Matsubara, H., & Hashimoto, T. 2004. SPIRAL1 encodes a plant-specific microtubule-localized protein required for directional control of rapidly expanding Arabidopsis cells. *The Plant Cell*, *16*(5), 1178-1190.

Nieminen, K., Immanen, J., Laxell, M., Kauppinen, L., Tarkowski, P., Dolezal, K., ... & Bhalerao, R. 2008. Cytokinin signaling regulates cambial development in poplar. *Proceedings of the National Academy of Sciences*, *105*(50), 20032-20037.

Nilsson, J., Karlberg, A., Antti, H., Lopez-Vernaza, M., Mellerowicz, E., Perrot-Rechenmann, C., ... & Bhalerao, R. P. 2008. Dissecting the molecular basis of the regulation of wood formation by auxin in hybrid aspen. *The Plant Cell*, *20*(4), 843-855.

Nuruzzaman, M., Manimekalai, R., Sharoni, A. M., Satoh, K., Kondoh, H., Ooka, H., & Kikuchi, S. 2010. Genome-wide analysis of NAC transcription factor family in rice. *Gene*, *465(1-2)*, 30-44.

Obaton, M. 1960. *Les Lianes ligneuses a structure anormale des forêts denses d'Afrique occidentale: thèse...* Masson & Cie.

Ohashi-Ito, K., & Fukuda, H. 2003. HD-Zip III homeobox genes that include a novel member, ZeHB-13 (Zinnia)/ATHB-15 (Arabidopsis), are involved in procambium and xylem cell differentiation. *Plant and Cell Physiology*, *44*(12), 1350-1358.

Olson, M. E., Anfodillo, T., Rosell, J. A., Petit, G., Crivellaro, A., Isnard, S., ... & Castorena, M. 2014. Universal hydraulics of the flowering plants: vessel diameter scales with stem length across angiosperm lineages, habits and climates. *Ecology Letters*, *17*(8), 988-997.

Pace, M. R., Alcantara, S., Lohmann, L. G., & Angyalossy, V. 2015a. Secondary phloem diversity and evolution in Bignonieae (Bignoniaceae). *Annals of botany*, *116*(3), 333-358.

Pace, M. R., & Angyalossy, V. 2013. Wood anatomy and evolution: a case study in the Bignoniaceae. *International Journal of Plant Sciences*, *174*(7), 1014-1048.

Pace, M. R., Lohmann, L. G., Angyalossy, V. 2009. The rise & evolution of the cambial variant in Bignonieae. *Evolution & Development, 11*, 465-479.

Pace, M. R., Lohmann, L. G., Angyalossy, V. 2011. Evolution of disparity between the regular & variant phloem in Bignonieae (Bignoniaceae). *American Journal of Botany, 98*, 602-618.

Pace, M. R., Lohmann, L. G., Olmstead, R. G., & Angyalossy, V. 2015b. Wood anatomy of major Bignoniaceae clades. *Plant Systematics and Evolution*, *301*(3), 967-995.

Pace, M. R., Zuntini, A. R., Lohmann, L. G., & Angyalossy, V. 2016. Phylogenetic relationships of enigmatic Sphingiphila (Bignoniaceae) based on molecular and wood anatomical data. *Taxon*, *65*(5), 1050-1063.

Patro, R., Duggal, G., Love, M. I., Irizarry, R. A., & Kingsford, C. 2017. Salmon provides fast and bias-aware quantification of transcript expression. *Nature methods*, *14*(4), 417.

Petit, G., & Anfodillo, T. 2009. Plant physiology in theory and practice: an analysis of the WBE model for vascular plants. *Journal of Theoretical Biology*, *259*(1), 1-4.

Petit, G., & Anfodillo, T. 2011. Comment on "The blind men and the elephant: the impact of context and scale in evaluating conflicts between plant hydraulic safety and efficiency" by Meinzer et al.(2010). *Oecologia*, *165*(2), 271-274.

Pinheiro, J., Bates, D., DebRoy, S., Sarkar, D., Heisterkamp, S., Van Willigen, B., & Maintainer, R. 2017. Package 'nlme'. *Linear and Nonlinear Mixed Effects Models, version*, 3-1.

Poorter, L., McDonald, I., Alarcón, A., Fichtler, E., Licona, J. C., Peña-Claros, M., ... & Sass-Klaassen, U. 2010. The importance of wood traits and hydraulic conductance for the performance and life history strategies of 42 rainforest tree species. *New phytologist*, *185*(2), 481-492.

Putz, F. E. 1984. The natural history of lianas on Barro Colorado Island, Panama. *Ecology*, *65*(6), 1713-1724.

Quast, C., Pruesse, E., Yilmaz, P., Gerken, J., Schweer, T., Yarza, P., ... & Glöckner, F. O. 2012. The **SILVA** ribosomal RNA gene database project: improved data processing and web-based tools. *Nucleic acids research*, *41*(1), 590-596.

R Core Team 2013. R: A language and environment for statistical computing. R Foundation for Statistical Computing, Vienna, Austria.

Rajput, K. S., Raole, V. M., & Gandhi, D. 2008. Radial secondary growth and formation of successive cambia and their products in Ipomoea hederifolia L.(Convolvulaceae). *Botanical journal of the Linnean Society*, *158*(1), 30-40.

Robinson, M., McCarthy, D., Chen, Y., & Smyth, G. K. 2010. edgeR: differential expression analysis of digital gene expression data. *J. Hosp. Palliat. Nurs*, *4*, 206-207.

Robinson, M. D., & Oshlack, A. 2010. A scaling normalization method for differential expression analysis of RNA-seq data. *Genome biology*, *11*(3), 25.

Robinson, M. D. & Smyth, G. K. 2008. Small-sample estimation of negative binomial dispersion, with applications to SAGE data. *Biostatistics, 9*, 21–332.

Robischon, M., Du, J., Miura, E., & Groover, A. 2011. The Populus class III HD ZIP, popREVOLUTA, influences cambium initiation and patterning of woody stems. *Plant physiology*, *155*(3), 1214-1225.

Rowe, N. P. & Speck, T. 1996. Biomechanical characteristics of the ontogeny & growth habit of the tropical liana Condylocarpon guianense (Apocynaceae). *International Journal of Plant Sciences, 157*,406-417.

Sachs, T. 1981. The control of the patterned differentiation of vascular tissues. In *Advances in botanical research*. Academic Press, 151-262.

Saez, A., Apostolova, N., Gonzalez-Guzman, M., Gonzalez-Garcia, M. P., Nicolas, C., Lorenzo, O., & Rodriguez, P. L. 2004. Gain-of-function and loss-of-function phenotypes of the protein phosphatase 2C HAB1 reveal its role as a negative regulator of abscisic acid signalling. *The Plant Journal*, *37*(3), 354-369.

Sahni, S., Prasad, B. D., Liu, Q., Grbic, V., Sharpe, A., Singh, S. P., & Krishna, P. 2016. Overexpression of the brassinosteroid biosynthetic gene DWF4 in Brassica napus simultaneously increases seed yield and stress tolerance. *Scientific reports*, *6*, 28298.

Sanchez-Moran, E., Osman, K., Higgins, J. D., Pradillo, M., Cunado, N., Jones, G. H., & Franklin, F. C. H. 2008. ASY1 coordinates early events in the plant meiotic recombination pathway. *Cytogenetic and genome research*, *120*(3-4), 302-312.

Scarpella, E., Marcos, D., Friml, J., & Berleth, T. 2006. Control of leaf vascular patterning by polar auxin transport. *Genes & development*, *20*(8), 1015-1027.

Schenck, H. 1893. Beiträge zur Biologie und Anatomie der Lianen im Besonderen der in Brasilien einheimischen Arten. In Schimper, A. F. W. (ed.). Beiträge zur Anatomie der Lianen: Botanische Mittheilungen aus den Tropen. G Fischer, Jena.

Schneider, C. A., Rasband, W. S., & Eliceiri, K. W. 2012. NIH Image to ImageJ: 25 years of image analysis. *Nature methods*, *9*(7), 671.

Scholz, A., Klepsch, M., Karimi, Z., & Jansen, S. 2013. How to quantify conduits in wood?. *Frontiers in Plant Science*, *4*, 56.

Smetana, O., Mäkilä, R., Lyu, M., Amiryousefi, A., Rodriguez, F. S., Wu, M. F., ... & Roszak, P. 2019. High levels of auxin signalling define the stem-cell organizer of the vascular cambium. *Nature*, *565*(7740), 485.

Smyth, D. R. 2016. Helical growth in plant organs: mechanisms and significance. *Development*, *143*(18), 3272-3282.

Snow, R. 1935. Activation of cambial growth by pure hormones. *New Phytologist*, *34*(5), 347-360.

Soler, M., Camargo, E. L. O., Carocha, V., Cassan-Wang, H., San Clemente, H., Savelli, B., ... & Grima-Pettenati, J. 2015. The E ucalyptus grandis R 2 R 3-MYB transcription factor family: evidence for woody growth-related evolution and function. *New Phytologist, 206(4)*, 1364-1377.

Sousa-Baena, M. S., Lohmann, L. G., Rossi, M., & Sinha, N. R. 2014a. Acquisition and diversification of tendrilled leaves in Bignonieae (Bignoniaceae) involved changes in expression patterns of SHOOTMERISTEMLESS (STM), LEAFY/FLORICAULA (LFY/FLO), and PHANTASTICA (PHAN). *New Phytologist*, *201*(3), 993-1008.

Sousa-Baena, M. S., Sinha, N. R., & Lohmann, L. G. 2014b. Evolution and Development of Tendrils in Bignonieae (Lamiales, Bignoniaceae) 1. *Annals of the Missouri Botanical Garden*, *99*(3), 323-348.

Sperry, J. S., Meinzer, F. C., & McCULLOH, K. A. 2008. Safety and efficiency conflicts in hydraulic architecture: scaling from tissues to trees. *Plant, Cell & Environment*, *31*(5), 632-645.

Sperry, J. S., Smith, D. D., Savage, V. M., Enquist, B. J., McCulloh, K. A., Reich, P. B., ... & von Allmen, E. I. 2012. A species-level model for metabolic scaling in trees I. Exploring boundaries to scaling space within and across species. *Functional Ecology*, *26*(5), 1054-1065.

Steppe, K., & Lemeur, R. 2007. Effects of ring-porous and diffuse-porous stem wood anatomy on the hydraulic parameters used in a water flow and storage model. *Tree physiology*, *27*(1), 43-52.

Sundell, D., Street, N. R., Kumar, M., Mellerowicz, E. J., Kucukoglu, M., Johnsson, C., ... & Tuominen, H. 2017. AspWood: high-spatial-resolution transcriptome profiles reveal uncharacterized modularity of wood formation in Populus tremula. *The Plant Cell*, *29*(7), 1585-1604.

Tamaio, N., Joffily, A., Braga, J. M. A., & Rajput, K. S. 2010. Stem anatomy and pattern of secondary growth in some herbaceous vine species of Menispermaceae. *The Journal of the Torrey Botanical Society*, *137*(2), 157-166.

Taylor, N. G., Howells, R. M., Huttly, A. K., Vickers, K., & Turner, S. R. 2003. Interactions among three distinct CesA proteins essential for cellulose synthesis. *Proceedings of the National Academy of Sciences*, *100*(3), 1450-1455.

Thode, V. A., Sanmartín, I., & Lohmann, L. G. 2019. Contrasting patterns of diversification between Amazonian and Atlantic forest clades of Neotropical lianas (Amphilophium, Bignonieae) inferred from plastid genomic data. *Molecular phylogenetics and evolution*, *133*, 92-106.

Torres, C. A., Zamora, C. M. P., Nuñez, M. B., & Gonzalez, A. M. 2018. In vitro antioxidant, antilipoxygenase and antimicrobial activities of extracts from seven climbing plants belonging to the Bignoniaceae. *Journal of integrative medicine*, *16*(4), 255-262.

Torrey, J. G., & Loomis, R. S. 1967. Auxin-cytokinin control of secondary vascular tissue formation in isolated roots of Raphanus. *American Journal of Botany*, *54*(9), 1098-1106.

Tuominen, H., Puech, L., Fink, S., & Sundberg, B. 1997. A radial concentration gradient of indole-3-acetic acid is related to secondary xylem development in hybrid aspen. *Plant Physiology*, *115*(2), 577-585.

Tyree, M. T., Davis, S. D., & Cochard, H. 1994. Biophysical perspectives of xylem evolution: is there a tradeoff of hydraulic efficiency for vulnerability to dysfunction?. *IAWA journal*, *15*(4), 335-360.

Tyree, M. T., & Ewers, F. W. 1991. The hydraulic architecture of trees and other woody plants. *New Phytologist*, *119*(3), 345-360.

Tyree, M. T., & Zimmermann, M. H. 2002. Hydraulic architecture of whole plants and plant performance. In *Xylem structure and the ascent of sap*. Springer, Berlin, Heidelberg. 175-214.

Uggla, C., Moritz, T., Sandberg, G., & Sundberg, B. 1996. Auxin as a positional signal in pattern formation in plants. *Proceedings of the national academy of sciences*, *93*(17), 9282-9286.

Valdivia, E. R., Herrera, M. T., Gianzo, C., Fidalgo, J., Revilla, G., Zarra, I., & Sampedro, J. 2013. Regulation of secondary wall synthesis and cell death by NAC transcription factors in the monocot Brachypodium distachyon. *Journal of experimental botany*, *64(5)*, 1333-1343.

Vanstraelen, M., Inzé, D., & Geelen, D. 2006. Mitosis-specific kinesins in Arabidopsis. *Trends in plant science*, *11*(4), 167-175.

Victorio MP. 2016. Roots and stems anatomy of Bignonieae: lianescent syndrome and secondary xylem. MSc dissertation, University of São Paulo, São Paulo, Brazil.

Vieten, A., Vanneste, S., Wiśniewska, J., Benková, E., Benjamins, R., Beeckman, T., ... & Friml, J. 2005. Functional redundancy of PIN proteins is accompanied by auxin-dependent cross-regulation of PIN expression. *Development*, *132*(20), 4521-4531.

West, G. B., Brown, J. H., & Enquist, B. J. 1999. A general model for the structure and allometry of plant vascular systems. *Nature*, *400*(6745), 664.

Wang, Z., Gerstein, M., & Snyder, M. 2009. RNA-Seq: a revolutionary tool for transcriptomics. *Nature reviews genetics*, *10*(1), 57.

Wyka, T. P., Zadworny, M., Mucha, J., Żytkowiak, R., Nowak, K., & Oleksyn, J. 2019. Species-specific responses of growth and biomass distribution to trellis availability in three temperate lianas. *Trees*, *33*(3), 921-932.

Xu, P., Kong, Y., Song, D., Huang, C., Li, X., & Li, L. 2014. Conservation and functional influence of alternative splicing in wood formation of Populus and Eucalyptus. *BMC genomics*, *15*(1), 780.

Yamamoto, R., Demura, T., & Fukuda, H. 1997. Brassinosteroids induce entry into the final stage of tracheary element differentiation in cultured Zinnia cells. *Plant and Cell Physiology*, *38*(8), 980-983.

Yamamoto, R., Fujioka, S., Demura, T., Takatsuto, S., Yoshida, S., & Fukuda, H. 2001. Brassinosteroid levels increase drastically prior to morphogenesis of tracheary elements. *Plant Physiology*, *125*(2), 556-563.

Yang, C., Song, J., Ferguson, A. C., Klisch, D., Simpson, K., Mo, R., ... & Wilson, Z. A. 2017. Transcription factor MYB26 is key to spatial specificity in anther secondary thickening formation. *Plant physiology*, *175*(1), 333-350.

Yang, C., Xu, Z., Song, J., Conner, K., Barrena, G. V., & Wilson, Z. A. 2007. Arabidopsis MYB26/MALE STERILE35 regulates secondary thickening in the endothecium and is essential for anther dehiscence. *The Plant Cell*, *19*(2), 534-548.

Ye, Z. H., & Zhong, R. 2015. Molecular control of wood formation in trees. *Journal of experimental botany*, *66*(14), 4119-4131.

Yoshida, T., Nishimura, N., Kitahata, N., Kuromori, T., Ito, T., Asami, T., ... & Hirayama, T. 2006. ABA-hypersensitive germination3 encodes a protein phosphatase 2C (AtPP2CA) that strongly regulates abscisic acid signaling during germination among Arabidopsis protein phosphatase 2Cs. *Plant physiology*, *140*(1), 115-126.

Zamariola, L., De Storme, N., Vannerum, K., Vandepoele, K., Armstrong, S. J., Franklin, F. C. H., & Geelen, D. 2014. SHUGOSHIN s and PATRONUS protect meiotic centromere cohesion in A rabidopsis thaliana. *The Plant Journal*, *77*(5), 782-794.

Zhang, J., Eswaran, G., Alonso-Serra, J., Kucukoglu, M., Xiang, J., Yang, W., ... & Yun, J. Y. 2019. Transcriptional regulatory framework for vascular cambium development in Arabidopsis roots. *Nature plants*, *5*(10), 1033-1042.

Zhang, Q., Luo, F., Zhong, Y., He, J., & Li, L. 2019. Modulation of NST1 activity by XND1 regulates secondary cell wall formation in Arabidopsis thaliana. *Journal of experimental botany*.

Zhang, J., Nieminen, K., Serra, J. A. A., & Helariutta, Y. 2014. The formation of wood and its control. *Current opinion in plant biology*, *17*, 56-63.

Zhao, C., Avci, U., Grant, E. H., Haigler, C. H., & Beers, E. P. 2008. XND1, a member of the NAC domain family in Arabidopsis thaliana, negatively regulates lignocellulose synthesis and programmed cell death in xylem. *The Plant Journal*, *53*(3), 425-436.

Zhbannikov, I. Y., Hunter, S. S., Foster, J. A., & Settles, M. L. 2017. SeqyClean: a pipeline for high-throughput sequence data preprocessing. In *Proceedings of the 8th ACM International*

Conference on Bioinformatics, Computational Biology, and Health Informatics (pp. 407-416). ACM.

Zhong, R., Demura, T., & Ye, Z. H. 2006. SND1, a NAC domain transcription factor, is a key regulator of secondary wall synthesis in fibers of Arabidopsis. *The Plant Cell*, *18*(11), 3158-3170.

Zhong, R., Lee, C., McCarthy, R. L., Reeves, C. K., Jones, E. G., & Ye, Z. H. 2011. Transcriptional activation of secondary wall biosynthesis by rice and maize NAC and MYB transcription factors. Plant and Cell Physiology, 52(10), 1856-1871.

Zhong, R., Lee, C., & Ye, Z. H. 2010. Functional characterization of poplar wood-associated NAC domain transcription factors. Plant Physiology, 152(2), 1044-1055.

Ziemińska, K., Butler, D. W., Gleason, S. M., Wright, I. J., & Westoby, M. 2013. Fibre wall and lumen fractions drive wood density variation across 24 Australian angiosperms. *AoB Plants*, *5*.

Ziemińska, K., Westoby, M., & Wright, I. J. 2015. Broad anatomical variation within a narrow wood density range—a study of twig wood across 69 Australian angiosperms. *PLoS One*, *10*(4), e0124892.

Zimmermann, M. H. 1983. Xylem structure and the ascent of sap. Springer, Berlin.

Zinkgraf, M., Gerttula, S., & Groover, A. 2017. Transcript profiling of a novel plant meristem, the monocot cambium. *Journal of integrative plant biology*, *59*(6), 436-449.

Supporting Information

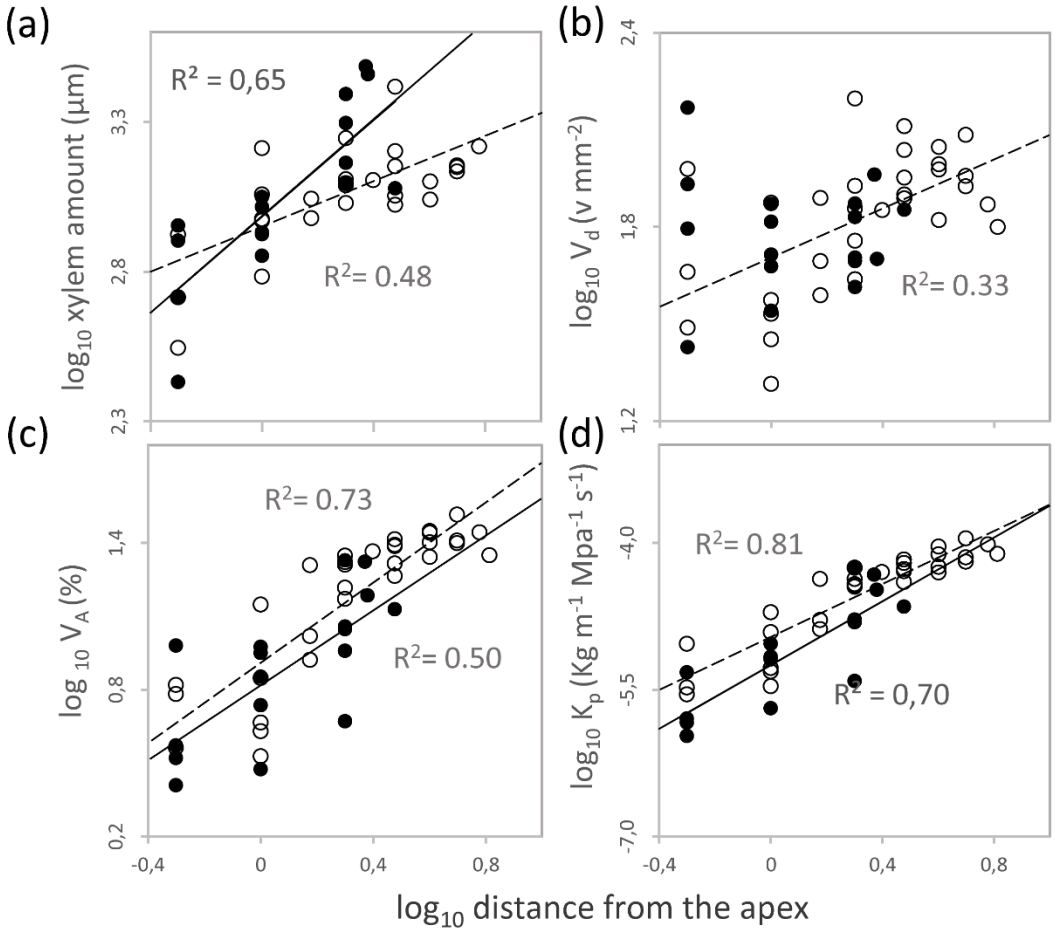

Supporting Information Fig. S1. Linear regressions of $\log_{10}$ transformed data of hydraulic parameters along the stems grown with and without support. **(a)** Amount of xylem produced by the cambium. **(b)** Vessel density. **(c)** Proportion of vessel area. **(d)** Potential water conductivity. Open circles refer to stems grown with support; black circles refer to stems grown without support; dashed lines: significant ($p \leq 0.001$) regression lines of supported stems data; solid lines: significant ($p \leq 0.001$) regression lines of unsupported stems data.

Supporting Information Table S1. Statistical data summary of mixed effect linear models between hydraulic parameters and distance from stem apex. Estimated bold coefficients are significant. coef: coeficiente; SE: standard error; DF: degrees of freedom.

	coef	SE	DF	t-value	p-value	Random effect	
						Individual	Residual
Xylem amount							
Supported stems						0.13	0.05
Intercept	**2.94**	0.03	34	85.20	<0.001		
Length	**0.51**	0.06	34	8.11	<0.001		
Unsupported stems						0.16	0.06
Intercept	**3.01**	0.04	18	68.25	<0.001		
Length	**0.89**	0.14	18	6.41	<0.001		
Vessel density							
Supported stems						0.28	0.33
Intercept	**3.91**	0.15	25	25.61	<0.001		
Length	**0.45**	0.09	25	5.15	<0.001		
Unsupported stems						0.08	0.40
Intercept	**4.09**	0.11	11	37.51	<0.001		
Length	-0.03	0.16	11	-0.20	0.85		
Vessel hydraulic diameter							
Supported stems						0,03	0,04
Intercept	**1.73**	0.02	25	96.85	<0.001		
Length	**0.24**	0.02	25	11.20	<0.001		
Unsupported stems						0.01	0.07
Intercept	**1.65**	0.02	11	89.00	<0.001		
Length	**0.41**	0.06	11	6.45	<0.001		
Vessel area proportion							
Supported stems						0.06	0.14
Intercept	**0.92**	0.05	25	19.52	<0.001		
Length	**0.83**	0.09	25	9.78	<0.001		
Unsupported stems						0.16	0.14
Intercept	**0.82**	0.09	11	10.06	<0.001		
Length	**0.71**	0.14	11	5.15	0.003		
Potential conductivity							
Supported stems						0.10	0.19
Intercept	**-9.97**	0.07	25	-76.52	<0.001		
Length	**1.37**	0.11	25	12.27	<0.001		
Unsupported stems						0.20	0.23
Intercept	**-5.26**	0.	11	-48.40	<0.001		
Length	**1.56**	0.22	11	7.15	<0.001		

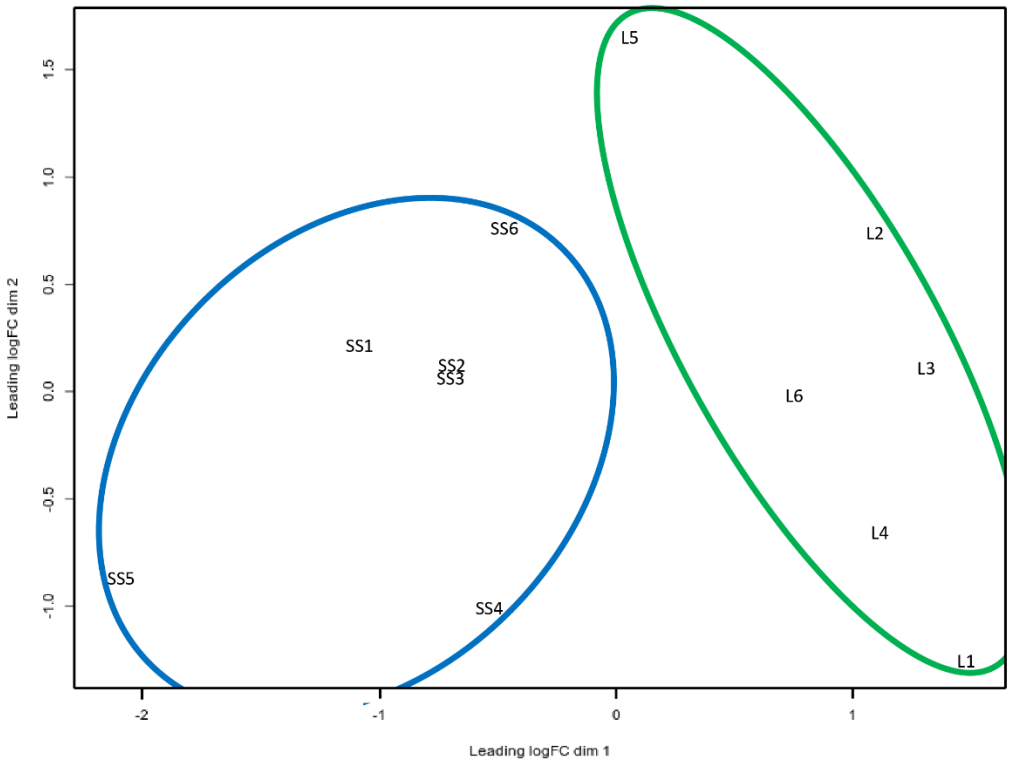

Supporting Information Fig. S2 Multidimensional scaling plot (MDS) showing samples expression profile similarity.